NBSIR 74-480 (R)

Evaluation and Calibration of Mechanical Shock Accelerometers by Comparison Methods

John D. Ramboz. Charles Federman

Vibration Section, Mechanics Division
Institute for Basic Standards
National Bureau of Standards
Washington, D. C. 20234

March 1974

Final Report

Prepared for

Department of Defense
Calibration Coordination Group

NBSIR 74-480

EVALUATION AND CALIBRATION OF MECHANICAL SHOCK ACCELEROMETERS BY COMPARISON METHODS

John D. Ramboz, Charles Federman

Vibration Section, Mechanics Division
Institute for Basic Standards
National Bureau of Standards
Washington, D. C. 20234

March 1974

Final Report

Prepared for
Department of Defense
Calibration Coordination Group

U. S. DEPARTMENT OF COMMERCE, Frederick B. Dent, Secretary

NATIONAL BUREAU OF STANDARDS, Richard W. Roberts, Director

FOREWORD

The evaluation of the shock accelerometers discussed in this report was sponsored by the Department of Defense Calibration Coordination Group (DoD/CCG) consisting of: the Metrology Engineering Center, Bureau of Naval Weapons Representative, Pomona, California 91766; the Aerospace Guidance and Metrology Center, Newark Air Force Station, Newark, Ohio 43055; and the Metrology and Calibration Center, Redstone Arsenal, Alabama 35809. The Atomic Energy Commission was represented by an observer from the Sandia Laboratory, Albuquerque, New Mexico 87115.

The Dod/CCG project number assigned was CCG 72-64 and work was performed under NBS cost center 2130426.

TABLE OF CONTENTS

LIST OF TABLES

LIST OF FIGURES

APPENDICES

EVALUATION AND CALIBRATION OF MECHANICAL SHOCK ACCELEROMETERS BY COMPARISON METHODS

by

John D. Ramboz

and

Charles Federman

ABSTRACT

A means to calibrate mechanical shock accelerometers by a comparison method has been developed. Detailed procedures and equipment used to generate mechanical shock pulses, collect data, and analyze the results are discussed. Three accelerometers were subjected to haversine acceleration-time pulses of 50, 500, 900 and 1500 g peak amplitudes and time durations of 8.5, 1.2, 1.0, and 0.7 ms, respectively. Both time- and frequency-domain calibrations were performed. The shock calibrations agreed with sinusoidal values to within a few percent. Problems encountered and future developments are discussed.

UNITS OF MEASURE

In this report, SI units are used throughout with the exception of acceleration which is expressed in gravitational units of g. Also, all screw threads were a fine thread series and are designated by their screw size number and the pitch in numbers of threads per linear inch. This was done to facilitate communication with intended readers. Conversion to SI units may be accomplished using the following relationships: 1 g = 9.807 m/s^2; 1 in = 2.540 cm; and 1 deg = (π/180) rad.

KEYWORDS: Accelerometer, calibration, comparison reference, mechanical shock, shock generation, shock pickup, vibration.

1. INTRODUCTION

There is a demonstrated need to measure mechanical shock accurately over a wide range of amplitudes and wave forms. The improved design of structures to withstand such loads and the efficient use of energy for forming materials are only two of the more obvious benefits of a knowledge of shock accelerations and their effects.

One of the problems in measuring mechanical shock has been the inability to evaluate and calibrate shock measuring systems in the frequency domain, except by subjecting them to intense, steady state, sinusoidal motion at a few discrete frequencies. Such calibrations are inherently suspect because they are not characteristic of the environment to be measured, and transducers are frequently damaged during such tests. Sinusoidal calibrations of this nature are often time consuming and expensive. Shock measuring transducers can also be calibrated by measuring lumped response integrated over the total energy spectrum with no attempt to determine response as a function of frequency.

This report describes an investigation and evaluation of comparison methods for the calibration of accelerometers used for mechanical shock measurements. The accelerometers used were piezoelectric types, but others, such as the piezoresistive type, should pose no special problems. Two of the accelerometers were of the same manufacturer and model, and of a "single-ended, top-connector" shear design. A third accelerometer was a "piggy-back" comparison standard of the compression design. Charge sensing was used throughout. Shock pulses were generated by a pneumatic shock test machine. See figure 1.

Comparison measurements were made in both the time and frequency comains. For the time domain analyses, comparisons were made by the peak ratio, the area ratio and instantaneous ratio methods. For the frequency domain analysis, the accelerometer's response is transformed from the time domain to the frequency domain through the use of a Fast Fourier Transform (FFT) algorithm. Ratios of transforms lead to the comparison calibration of one accelerometer in terms of another. The frequency domain analysis yields the solution in complex terms, i.e., amplitude and phase angle.

2. LABORATORY TEST MATRIX

Three accelerometers were used in these tests. For purposes of this report, the accelerometers are identified as A, B, and R. Units A and B are nominally identical while unit R is considered as a comparison reference. Laboratory measurements were made by comparing A to R, B to R, and A to B. This gives three basic accelerometer combinations.

The nominal amplitudes and durations of the pulses were:

Peak Acceleration	Impact Duration
50 g	8.5 ms
500 g	1.2 ms
900 g	1.0 ms
1500 g	0.7 ms

Table I shows the test matrix used. The notation, for example, of A/R indicates that accelerometer A was compared to accelerometer R, etc. For any one set of conditions, there were five repeated shock pulses made. This is indicated by the test number groups. In all, there were 60 pulses produced, 15 for each of the four shock conditions, five for each of the accelerometer combinations.

3. SHOCK PULSE CHARACTERISTICS

A perfectly elastic impact onto a linear spring would generate an ideal half-sine acceleration wave shape. However, because of nonlinearities and losses, the pulses generated in the laboratory take on the characteristics of a degraded half-sine and appear similar to a haversine function.

Though the description of wave shape is qualitatively called haversine, there are subtle differences in the time domain between a haversine and other similar shapes such as so called half-sine or Gaussian pulses. Ideally, the accelerometer calibration process should not be critically affected by the wave shape, although there are problems in the analysis for certain wave shapes. This is more fully discussed in Section 5.4.

Typical shock pulses are shown in figures 2a, 2b, 2c and 2d, and are from one channel of the two used for test data in this report. They were selected from accelerometer B, test number 4; test number 16; test number 31; and test number 46, respectively. These are samples from the 50 g, 500 g, 900 g, and 1500 g peak accelerations. The pulses measured with the other channel were quite similar to these samples.

Table II shows measured values of the pulse amplitudes and durations for the representative tests listed. In all instances, the measured amplitudes were within $\pm$15 percent of the nominal values. Because the calibration results are not a critical function of the shock amplitude, no special care was taken to maintain any better control of the amplitude.

4. PHYSICAL DESCRIPTION OF THE EQUIPMENT

The laboratory equipment consists of four main items: (1) a mechanical shock generating machine, (2) acceleration measuring transducers, (3) a data transfer system, and (4) a minicomputer for data storage and manipulation. These items provide a means for transient data generation, data collection and reduction, and calibration of test accelerometers.

4.1 Shock Test Machine

Mechanical shock pulses are generated in the laboratory with the use of an AVCO SM-105-2 Shock Test Machine [1]. This device is pneumatically controlled and actuated, with the capability of producing a variety of shock pulses up to 10,000 g. The device can be adjusted to produce those pulse shapes called out in established specifications [2-4]. A base, pneumatic cylinder, brake, carriage, control panel, and plate assembly make up the six major structural units of the machine. Shock pulse levels can be set rapidly by a simple adjustment of an air pressure regulator. An exploded view of the shock test machine is shown in figure 3.

A concrete filled, reinforced, steel shell serves as a seismic mass which, because of the mass, absorbs the impact of the carriage. Air reservoirs, built into the base, maintain four air-type shock mounts which support the block, so that only a small amount of energy is transmitted to the floor during impact. This design produces a low natural frequency which is excellent for mechanical shock isolation. The brake and cylinder assemblies are housed in the base assembly. Air pressure in the pneumatic cylinder is operator controlled to produce a range of forcing functions. The brake assembly stops the carriage after impact to eliminate multiple rebounds, and also holds and releases the carriage at the top of the stroke before the impact. A solid, integral, aluminum casting is used for the carriage. It is attached to the steel impact plate of the piston rod assembly, with guides attached to the back side to keep the carriage from turning. This guide also makes contact with the top and bottom limit switches which control the drop height, brake actuation, and trigger pulse initiation. The carriage and impact plate, as a unit, are forced down by air pressure onto any of a number of elastomer pads which are bolted to the base assembly.

The principle of operation is to suddenly drive a carriage into a spring element which decelerates the carriage, and then rebounds in the opposite direction. The shock amplitudes, durations, and shapes are controlled by the impacting medium, air pressure, and drop height. For all the tests in this report, only elastomer pads were used. Initial height and air pressure were adjusted to trim the shock pulse to the desired amplitude and duration. The accelerometers all gave negative outputs for the mechanical shocks because of the direction of the accelerometers mounting. A short time after the rebound, a pneumatic brake is applied which then brings the table to a controlled stop.

---

[1] Numerals in brackets refer to references found at the end of this report.

4.2 Acceleration Measuring Transducers

4.2.1 Reference System. The reference system consists of a reference accelerometer and a matched solid-state charge amplifier. Because the accelerometer is of the "piggy-back" configuration, other test accelerometers can be flush mounted to its top without the requirement of an additional fixture (see figure 4). This permits calibration by the comparison method, where the electrical outputs of the reference accelerometer and test accelerometer are compared, while both are subjected to the same motion. The accuracy of this method is directly dependent on the accuracy of the calibrated reference.

Use of a piezoelectric element in the reference accelerometer permits a flat temperature response and stability with time. An insulating, integral mounting stud isolates the crystal and the case from the surface upon which it is mounted. Erroneous signals generated by ground loops are minimized by use of a knurled nut on the output connector of the accelerometer. This feature allows connection or isolation of the signal ground from the case, thus providing a means of separating the reference and test signal grounds, and can also insure that the accelerometer cases are always connected to ground. The case of the reference accelerometer provides mechanical strain isolation for the piezoelectric element.

Output voltages of the reference charge amplifier are directly proportional to the charge generated by the reference accelerometer. This single-ended output had one side connected to circuit ground. According to the manufacturer, variations in the length of the cable between the accelerometer and the amplifier does not significantly affect the system sensitivity. The manufacturer lists the harmonic distortion of the amplifier as less than 0.2 percent with a frequency response of ± 0.5 percent from 10 to 10,000 Hz (100 Hz reference). It is also stated that the gain stability varies within ± 0.1 percent change with variations in line voltage over the range 105 to 125 vac. There is less than 0.1 percent change in gain 1000 pF change in source capacitance, according to the manufacturers' specifications.

This accelerometer-amplifier reference system was calibrated at the National Bureau of Standards. Both sinusoidal and interferometric methods were used for calibration of the system.

4.2.2 Test Accelerometer Pickup Characteristics. Two identical, high resonance frequency, shock accelerometers were used as the test accelerometers. Their small size, compact construction, stable operation, and high resonance frequency (approximately 80,000 Hz) makes them useful devices for measuring shock transients. The manufacturer's specifications for the two accelerometers claim a measurement capability of 20,000 g. They are self-generating, shear design, piezoelectric transducers requiring no power for operation.

During the testing sequence, an insulated mounting stud was placed under one of the test accelerometers when they were placed side by side. This procedure was done to insure electrical integrity between the two pickups.

The manufacturer's specifications list these transducers as having a nominal charge sensitivity of 0.7 pC/g. Other stated characteristics include a nominal voltage sensitivity (with 300 pF external capacitance) of 0.65 mV/g, a flat frequency response of 2 to 15,000 Hz, and a nominal transducer capacitance of 800 pF.

Physically, the transducers have an electrically grounded case made of 300 series stainless steel. Mounting to a surface is achieved by the use of a 10-32 UNF threaded hole in the base of the accelerometers. A torque of 2 Nm was used in mounting. The output connector is located on top of the case, and has 10-32 UNF threads, which mates with a miniature coaxial cable. The complete accelerometer unit is epoxy sealed. Additional specifications are listed in appendix A.

4.3 Analog-To-Digital Converter and Interface Control System

The analog-to-digital converter and interface control system (ADC-ICS) serves as an interface between the data generation and data collection cycles. Data, in the form of analog voltages, is converted and transferred via the ADC-ICS, from the accelerometer systems to a minicomputer.

An operator controlled initiation switch, on the front panel of the ADC-ICS, activates the unit and turns on a ready status light. It then waits until it is triggered before the next data collection cycle begins.

During the data collection cycle, two multiplexed channels are outputed to the minicomputer. This puts a restriction on the data in that points from each channel are not time coincident. Thus a digitization phase error is produced which is corrected for in the final analysis.

4.3.1 Analog-To-Digital Converter (ADC). High-speed and high accuracy are combined, through the use of compact solid-state electronics in the ADC, to convert an analog input signal to an equivalent 14-bit plus sign output digital word. A combined parallel-decision/serial-correction technique is used as the method of conversion. Conversion rates of up to 250,000 conversions per second are obtained using this technique.

4.3.2 Interface Control System (ICS). The ICS section provides all the signals required by the ADC to convert an analog input voltage to a 14-bit plus sign digital word. An updated 16-bit address word is generated for each conversion. This address is used to indicate in which memory address the data word is to be stored. The initial memory location is set by front panel switches. The multiplexed data word and address are sent over the same set of transmission lines to the minicomputer. This unit is triggered by the trigger switch on the shock generating machine shortly before the shock pulse occurs.

4.4 Data Collection Device

A 16 k-byte core memory Interdata 3 minicomputer controls the data collection sequence of the calibration process. The memory is directly addressable with the primary instruction word. Sixteen general registers of 16 bits each can be used as index registers or accumulators. Shock data is sent by the ADC-ICS through the direct-memory-access port of the computer This method insures that all the transient data can be captured and stored in the core memory. After a block of data for a single run is stored in memory, it can be written on either paper or magnetic tape for future transfer to a larger computer for analysis.

4.5 Sequence of Test Events

Through the use of data provided by the manufacturer of the shock machine, the approximate pulse height and width is set by varying the drop height, air pressure, and combinations of elastomer pads. During a typical shock pulse measurement, the pneumatic shock machine is used to generate a shock pulse that is sensed by the reference and test accelerometers, which are mounted on the carriage. These transducers produce electrical signals proportional to the motion generated by the shock machine. The electrical signals are first amplified by charge amplifiers, and then the voltage analog outputs from these amplifiers are fed into variable gain voltage amplifiers. Figure 5 shows a block diagram of the equipment used.

As the carriage is on its down stroke, it activates a trigger switch just before the impact, which starts the data collection cycle in the ADC-ICS. At the same time, a transient recorder, monitoring both test and reference accelerometer signals, is activated to give the operator a refreshed trace (of the shock pulse as sensed by the transducers) on an oscilloscope.

After the ADC-ICS is triggered, it multiplexes and converts the data from the accelerometers, and sends this information to the minicomputer. While the data is still in the core memory, a software program is used to control an X-Y plotter to give a hard copy presentation of the shock pulse data. From here, the data is transferred to nine-track magnetic tape and taken to a larger computer for analysis.

5. DATA RECORDING AND ANALYSIS

5.1 General Discussion

The project goal was to determine the sensitivity factors of several accelerometers and determine an estimate of error of the comparison calibration process. This was done at several acceleration amplitudes and durations as previously discussed in Section 3.2. The shock pulse results were compared to values obtained by established sinusoidal calibration methods. Figure 6 shows the data processing steps between the laboratory test and the final results.

The figure is divided into five regions, one for each major area of data processing. The laboratory tests were conducted where the test data originated. One set was done by sinusoidal methods and the second by mechanical shock pulse tests. For part of the sinusoidal tests, a minicomputer was used for calibration control and data acquisition. For the shock pulse tests, a minicomputer was used as a fast digital data storage device. Some time-domain calculations were also made with the minicomputer.

The area identified as "large computer" is where the indicated involved calculations were performed. Shock data were transferred from the minicomputer to the large computer via magnetic tape. The large computer was used to calculate the Fast Fourier Transform (FFT), to curve fit the data, and to perform other calculations which will be subsequently discussed.

Post calculations were necessary and consisted of averaging data and applying correction factors for amplifier gains, filter phase shifts, etc. Finally, the data were put in tabular form and plots made. These will be individually discussed in later sections.

5.2 Sinusoidal Calibrations

5.2.1 Sinusoidal Calibration of Accelerometers A and B. Accelerometers A and B were calibrated by sinusoidal comparison methods, referenced to NBS vibration standards [5,6]. In April 1970, both were calibrated on Dimoff Vibration Standards D102, D201, and on the high-frequency interferometer facility [7,8,9]. Both were calibrated again in December 1972, on Dimoff Vibration Standards D102 and D201/203. An arbitrary weighted mean was calculated using the weighting factors shown in table III. More weight was given to the more recent calibrations.

A least squares fit was then made to the weighted mean data. The general shape of the sensitivity factor as a function of frequency is nearly exponential. At frequencies less than about 1750 Hz, the charge sensitivity decreases with increasing frequency.[10,11,12] At frequencies greater than about 5000 Hz, the sensitivity increases with increasing frequency due to mechanical resonance. In the frequency interval between 1750 and 5000 Hz, both effects cause the response to be nearly flat.

The sensitivity factors can be expressed as given below:

Accelerometer A,

$$S_a = 0.8827f^{-0.01102}, \quad 10 \leq f \leq 1750, \tag{1}$$

$$S_a = 0.8133 + 0.1810f \times 10^{-6}, \quad 1750 \leq f \leq 5000, \tag{2}$$

$$S_a = 0.4631f^{0.06637}, \quad 5000 \leq f \leq 10{,}000. \tag{3}$$

Accelerometer B,

$$S_b = 0.8586f^{-0.01082}, \quad 10 \leq f \leq 1750, \tag{4}$$

$$S_b = 0.7908 + 0.9564f \times 10^{-6}, \quad 1750 \leq f \leq 5000, \tag{5}$$

$$S_b = 0.4510f^{0.06688}, \quad 5000 \leq f \leq 10{,}000. \tag{6}$$

S_a and S_b are charge sensitivities of the accelerometers A and B, respectively, in units of pC/g, and f is the frequency in Hz. Table IV gives the weighted mean and fit values. The last decimal places are rounded approximations. The percent difference between the weighted mean and the fit value uses the fit value as a reference value, and was rounded to the nearest one-tenth percent. The maximum difference for either accelerometer was 0.7 percent, but in most instances was ±0.2 percent or less.

5.2.2 Sinusoidal Calibration of Accelerometer System R. The "piggy-back" accelerometer and its charge amplifier were calibrated as a system. It was done by a comparison method referenced to NBS Standard 1490 in April 1972. Two repeated runs were made on each of two vibration generators. Equal weighting was used in computing the mean. A least squares fit was made to the mean. The system sensitivity factors are given below:

Accelerometer System R,

$$S_r = 9.9586f^{2.3302\times10^{-4}}, \quad 30 \leq f \leq 4000, \tag{7}$$

$$S_r = 7.0736f^{4.0998\times10^{-2}}, \quad 4500 \leq f \leq 10{,}000. \tag{8}$$

S_r is the system sensitivity in units of mV/g and f is the frequency in Hz. Table IV gives the mean values and fit values. The last significant place is a rounded approximation. The percentage difference is rounded to the nearest one-tenth percent. The maximum difference was 0.7 percent, while in most instances the differences were ±0.2 percent or less.

5.3 Comparison Measurements in the Time Domain

5.3.1 Peak Comparison Method. A popular method for calibration of shock accelerometers is by the peak comparison method.[13,14] This has been even more useful in recent years with the availability of peak-holding meters. For these tests, the time domain data for each channel were printed out as part of the analysis. It is relatively easy to search for the maximum amplitude of the time domain signal for each of the two accelerometers being compared. This could have been done by the large computer, but was done manually.

The ratios of the peak values were calculated for each test of accelerometers A compared to R and B compared to R.(See table I.) The ratios from the repeated tests for any matching set of parameters were then averaged. This usually consisted of 5 repeated tests. The standard deviation was also calculated. The results are shown in table V.

The measured ratio of accelerometers A compared to B was also calculated and the results are shown in table V. The results of the time-domain measured ratios cannot be compared directly to other data because low-pass filters were used to improve the waveform. Analysis of comparison will be made in a later section of this report.

5.3.2 Instantaneous Ratio Comparison Method. Referring to figure 6, an instantaneous ratio of two accelerometers can be obtained by reading the data off the magnetic tape into the minicomputer and performing the necessary calculations. This could have also been done by the large computer. As shown in figure 5, an analog X-Y plotter was interfaced to the minicomputer.

Prior to and after the mechanical shock, the ratio is that of two noisy signals. The noise sources include mechanical vibration of the shock machine carriage, accelerometer cable noise, electronic noise from the amplifiers, stray pickup noise and possibly pyroelectric outputs from the accelerometers. In addition to these noises, any dc-offset voltages in the system from unbalanced amplifiers leads to inaccurate ratios. After the impact, over-shoot likewise leads to inaccurate ratios.

The only region that the instantaneous ratio becomes reliable is near the peak acceleration. As such, one could merely calculate the peak value as in Section 5.3.1. The general conclusion is that the method does yield a qualitative plot that is sometimes useful, but quantitative data are limited to only the values derived near the peak amplitudes.

5.3.3 Change-of-Velocity Comparisons. It is possible to compare the areas under the acceleration-time pulses. These areas are a measure of the change of velocity of the accelerometers under test. Ideally, the ratio of the velocities should lead to a satisfactory calibration process. In instances where there is minor ringing on the pulses, the area tends to average these effects. However, when there are dc off-sets or over-shoots involved, these can add significantly to the area. Additionally, the process becomes critical as to the time considered before and after the shock pulse because of the integration of off-sets and over-shoots.

For this project, the digitization "window" was always approximately 20 ms and the shock pulses were captured somewhere in this time interval. When the areas were computed large differences were apparent. For example, for the comparison of accelerometers B to R and for the five tests of 50 g, 8.5 ms, the mean peak ratio was 0.8024 while the mean area ratio was 0.7089, or about 11.7 percent less. Moreover, the standard deviation for the peak ratio comparison was about ±0.68 percent while the area ratios had a standard deviation of about ±3.31 percent.

Other examples could be cited, but the same general conclusion regarding these tests hold, namely, the area ratios are significantly lower than the peak ratios for the same tests and the area ratios have significantly larger standard deviations. Overall, this method cannot be recommended without more effort to refine the process.

5.4 Fast Fourier Transform Analysis

The Fourier Integral Transform is a mathematical operation which decomposes a time signal, in the form of a data array, into its complex frequency components (amplitude and phase). In order to efficiently analyze a transient shock pulse in the frequency domain, a high speed computational algorithm called the Fast Fourier Transform (FFT) is utilized in the calculation of the Fourier Integral Transform of a time signal. It is important to note that this mathematical process is not dependent upon any particular input pulse shape or waveform. But, for example, in transforming perfect half-sine and haversine pulses, the Fourier amplitudes go to zero at a number of frequency points, as shown in figures 7a and 7b respectively. The actual pulses generated in the laboratory had frequency components which came close, but did not go to zero over a long frequency span. A typical plot of transformed data can be found in figure 8.

A version of the Cooley-Tukey Fast Fourier Transform algorithm is used to analyze the shock pulse data [15]. (See Appendix B.) The program used works on a one-dimensional complex array, and outputs the Fourier real and imaginary frequency components in a similar array. This transform process is accomplished through the use of the UNIVAC 1108 Computer.

Data from each channel is reduced from 1024 real, time domain measurements to 512 complex frequency components. The frequency range obtainable (Nyquist folding frequency) is a direct function of the sampling rate [16]:

$$\text{Frequency Range} = (1/2)(\text{Sampling Rate}).$$

Resolution between frequency points is limited not only by the sampling rate, but also by the sample size:

$$\text{Resolution/Line} = (\text{Sample Rate})/(\text{Number of Data Points}).$$

For example, if the sample rate is 50 kHz and the number of samples taken is 1024:

$$\text{Frequency Range} = (1/2)(50\ \text{kHz}) = 25\ \text{kHz},$$

$$\text{Resolution/Line} = (50\ \text{kHz})/(1024\ \text{Points}) = 48.8\ \text{Hz/Point}.$$

This means that the data taken can be transformed into components out to 25 kHz in steps of 48.8 Hz.

5.4.1 Ratio of Transformed Data. After the time domain data from the test and reference accelerometers have been read from a nine-track magnetic tape, a software program transforms this data from the time to the frequency domain. Immediately after the transformation, this complex data output is converted to amplitude and phase relationships for the two transducers. The amplitude is obtained by taking the square root of the sum of the squares of the real and imaginary parts of each frequency component. For each discrete frequency point, the ratio is taken of the test and reference amplitudes. This ratio is then used as a base for calibration of the test accelerometer by comparison techniques.

5.4.2 Phase of Transformed Data. Phase information is calculated from the arctangent of the division: imaginary part divided by the real part. Then by using an identity for the conversion from radians to degrees, the phase angle is displayed as a positive or negative number of degrees from -90° to +90°. To determine the phase relationship between the two accelerometers, the calculated phase angle of the reference accelerometer is subtracted from the calculated test accelerometer phase angle. This result indicates whether the test accelerometer output is leading or lagging the reference accelerometer output.

5.5 Post Calculations

The post calculations consist of calculating averaged values of repeated tests, determining standard deviations of the repeated tests, averaging these results over selected frequency spans, and finally correcting the results for amplifier gain, filter response, and phase shift. These steps are shown in figure 6.

5.5.1 Test Ratio Means. The test mean is the unweighted average of the repeated tests performed for any one set of conditions. Generally, this was five repeated tests. In two instances, test data was lost during the overall process. These were test numbers 30 and 54, which resulted in a data set of four repeated tests for those two groups. Equation 9 below expresses the solution for the test means in general terms.

$$\overline{K}_t = \frac{\sum_{n=1}^{N} K_{tn}}{N} \quad , \tag{9}$$

where $\overline{K}_t$ = the test mean for any one frequency,

K_{tn} = the individual test ratios of the FFT amplitude at any one frequency, and

N = the number of repeated tests for any one combination of accelerometers.

5.5.2 Test Phase Means. The phase angle differences were averaged to yield an unweighted mean of the phase. The discussion in Section 5.6.1 applies to the test data. Equation 10 below expresses the solution for the phase mean in general terms.

$$\overline{\phi}_t = \frac{\sum_{n=1}^{N} \phi_{tn}}{N} \quad , \tag{10}$$

where $\overline{\phi}_t$ = the phase mean,

ϕ_{tn} = the individual phase differences of the FFT phases at any one frequency, and

N = as described for equation 9.

5.5.3 Standard Deviation. The standard deviations were calculated for the groups for which the means were calculated. For the test ratios, the standard deviations are all expressed in percent of the test mean. For the test phase, the standard deviation is expressed in degrees.

The statistical validity of standard deviation when only a few measurements are made is open to question. It does, however, give some measure of the quality of the measurement in a qualitative way.

5.5.4 Averaging Over Frequency Intervals. It is convenient to plot and examine the results on a logarithmic frequency scale. When this is done, it is not practical to plot at each frequency for frequencies much greater than 1 kHz or so. This, of course, depends on the frequency of the harmonics from the FFT. In order to summarize data, averaging over selected frequency ranges was done. In addition, it also serves to reduce the randomness of the data. The averaging, or more appropriately smoothing, over frequency was accomplished by averaging together the results for an arbitrary interval of frequency components.

The harmonic frequency (Δf) of the FFT for these tests was approximately 50 Hz. The data were averaged and are presented every 100 Hz for $600 \leq f \leq 1000$ Hz, every 250 Hz for $1250 \leq f \leq 2000$ Hz and every 500 Hz for $2500 \leq f \leq 5000$ Hz. No averaging over frequency was done below 500 Hz. Table VI shows these frequency ranges and the number of points that were included in the averages. At a frequency of 200 Hz and above, the plotted data is distributed at frequency intervals of between one-third and one-sixth octaves. For accelerometers having a relatively smooth response, this is adequate to describe their performance. If narrow band resonances were to occur, this method would have to be altered to keep from "averaging out" the effect of the resonance. No such resonances occurred in the data reported herein.

When considering the repeated tests and the frequency averaging as a whole, the total number of measurement values in the final average becomes sizeable above 1000 Hz. This makes the measurement statistics much more meaningful.

The standard deviations were "pooled" over the same frequency range as above. This process involved squaring each deviation, summing them, dividing by the number of points, and then extracting the square root. This is valid for equal sized samples.

5.5.5 Amplifier Gain Corrections. The amplifier gains for the two test accelerometer channels were divided out of the final results. This yields the sensitivity factor of the accelerometer in units of pC/g. Additionally, for those tests where a low pass filter was used, the amplitude response of the filter also was taken into account. Nominal values were used for the unfiltered gain. Measured values were used for the filter responses.

5.5.6 Phase Shift Corrections. Phase shifts originate in the measurement and analysis from the following sources:

1. Relative motion between the two accelerometers,
2. Mechanical time delay within the accelerometers,
3. Electronic time delay of the amplifiers,
4. Low-pass filter phase shift, and
5. Non-coincident digitization delay.

No analytical corrections can be made for phase shifts due to relative motion between the two accelerometers being tested. In a good back-to-back configuration, this effect should not be of any consequence at frequencies below about 3 to 5 kHz. However, when the accelerometers are mounted side-by-side, there could be significant problems due to rocking motions.

The phase shift due to mechanical time delay within the accelerometer, is of course, one of the parameters for which the test is being performed. For accelerometers having very low damping, the phase shifts are small until the accelerometer or other mechanical resonance is approached.

In a good quality, wide-band amplifier, the electronic phase shift is small. In ac-coupled amplifiers, shifts can occur at very low frequencies. Amplifier phase shift generally occurs as a constant time delay. This creates a lagging phase shift which varies linearily with frequency. No pulse distortion will result from this condition. Additionally, these shifts, even though small, can be measured and corrected for.

Low-pass filters usually create the largest phase shifts in typical systems. Once the filter characteristics are measured, this effect can be corrected out of the final measurement of the accelerometer sensitivity and phase. A low-pass filter always creates a phase lag condition by itself. However, because the accelerometer sensitivity results from a ratio, the filter can have an effect of either a lag or lead depending on whether the filter is in the channel that becomes the numerator or the denominator of the ratio calculation. Moreover, if a filter is used in both channels, then the difference of phase shift between the two filters can cause either a lag or lead phase condition.

A phase shift can also be synthesized into the process by non-coincident sampling of the two accelerometer outputs.[17] As was discussed in Section 4.2.1, the input of the analog-to-digital converter was multiplexed between the two accelerometer inputs. As such, channel 2 is measured at a slightly later time than channel 1. This length of time is equal to the reciprocal of the sampling rate. This time delay in this project was approximated 10μs. The uncorrected FFT assumes that coincident time sampling occurred. When coincidence is assumed, it appears that channel 1 lags channel 2 by 10μs. This phase shift is described by

$$\phi_m = \frac{180(\eta-1)}{N} = 360\left(\frac{f}{f_s}\right) \quad , \tag{11}$$

where ϕ_m = phase error in degrees due to multiplexing time delay (leading angle as described above),

η = harmonic line number from the FFT algorithm, (η=1 for f=0 Hz),

N = number of points sampled,

f = harmonic frequency, and

f_s = analog-to-digital sampling frequency.

For the testing described in this report, N=1024 points, and $f_s \approx 100$ kHz. Using these values,

$$\phi_m \approx 0.1758\ (\eta-1) \approx 0.0036\ f. \tag{12}$$

The correction of this synthesized error can be easily made. Because η and N are exact integers, and f_s and f can be measured with accuracy, ϕ_m can be computed to almost any required accuracy.

All the data presented in the next section were corrected for the phase shifts due to amplifier delay, filter shift, and the multiplexing shift.

6. DISCUSSION OF RESULTS

6.1 Sensitivity Results

6.1.1. Sensitivity Data and Plots. The sensitivity data for both accelerometers, tables VII and VIII, are plotted graphically in figures 9a and 9c, to get an overall view of the trends and limitations of the shock calibration process. On these same graphs, the fitted values for the sinusoidal calibrations are also plotted for reference purposes. The sensitivity data for each pickup are divided into separate acceleration levels: 50, 500, 900, and 1500 g.

Both figures have very similar characteristics, which is expected because the two accelerometers used are of the same manufacturer and configuration. For the 50 g curves, the sensitivity tends to drop off much sooner than the other acceleration levels. The drop off is readily seen to begin at approximately 300 Hz. This indicates that there is a lack of high frequency information in the 50 g pulse. The curves of sensitivity for the 500 and 900 g pulses are similar because there is not much difference in their acceleration waveforms. Both follow a smooth exponential curve until they reach the 2000 Hz frequency point, where the curves rise upward. One exception for this trend is the 500 g pulse of accelerometer B, which instead of rising at this point, falls to a lower level, and then rises at 3000 Hz. The 1500 g plotted sensitivity follows similar trends in the 500 to 5000 Hz ranges, but at the low frequency end, below 500 Hz, the data become erratic. This inconsistency shows that there was very little or poor low frequency information in the high g pulses.

6.1.2 Standard Deviation of Sensitivity Data. The plotted standard deviations of the sensitivity data, figures 9b and 9d, are directly related to the characteristics of the sensitivity plots. At the same frequency point where the sensitivity for an accelerometer falls or rises abruptly, the standard deviation rises. This is an indication of the points where the process breaks down because of the limitations in the frequency content of the shock pulses.

An unusual trend sets the 1500 g standard deviation plots at higher levels than the other plots. This difference is due to the fact that one out of the 5 sets of data has values which are far from the other four, over the complete frequency range plotted. Because this apparent shift shows up in both accelerometers A and B, it is considered a systematic error orginating in the laboratory.

6.2 Phase Component Results

6.2.1 Phase Data and Plots. Phase relationship data can be found in tables IX and X. These data are plotted in figures 9e and 9g to provide an overall view of the phase characteristics. Plots for each of the accelerations are found on the same graph. In phase response, as in the plots of sensitivity, the two accelerometers, A and B, have a resemblance, so that one description gives an overall view of both sets of data. It should be noted that this phase relationship is between the test accelerometer, either A or B, and the reference standard R.

The phase plots are flatter out to higher frequencies than the sensitivity curves. This indicates that the shape and frequency content of the pulse do not affect the phase as much as the accelerometer amplitude versus frequency. The 50 g level pulse is unstable after 300 Hz, but continues within 5 degrees of the other curves, while the others continue in a stable manner out to 2000 Hz.

6.2.2 Standard Deviation of Phase Data. Standard deviations for the phase components which are tabulated in terms of degrees, found in tables IX and X, show trends that are more stable than the standard deviations of the sensitivity data. Plots of the standard deviations of the phase data are found in figures 9f and 9h.

In both accelerometers the trends for standard deviations are similar. At approximately 300 Hz, the standard deviation for the 50 g level pulse rises. The other pulses are linear out to 2000 Hz, where, there too, the standard deviations rise. This rise is not as distinct on the 1500 g level pulse, since phase information from this pulse tends to be more stable at the higher frequencies.

6.3 Comparisons

6.3.1 Comparison to Sinusoidal Data. The curve fitted sinusoidal calibration data are listed in table IV, and plotted on figures 9a and 9c. As seen from the graphs, the sensitivities derived from the shock calibrations closely approximate the sine wave calibrations. In general, the values from the shock process tend to be lower than the sinusoidal until a point near 2000 Hz is reached. This trend of the shock data shows a constant difference of approximately one percent from the sinusoidal data over the frequency range from 50 to 2000 Hz. Inherent errors in the data processing or the laboratory measurement techniques can cause such errors as described above. The shock and sinusoidal data demonstrate graphically that two independent systems can provide accelerometer sensitivities to within ±1 percent of each other over long frequency intervals.

6.3.2 Comparison to Time Domain Data. There is an important distinction between the shock calibration results in the time domain and the frequency domain. All the calibration methods directly using time domain shock pulse measurements yield a single value of accelerometer sensitivity. For purposes of precision calibration, this is usually inadequate inasmuch as the accelerometer's sensitivity is not a constant value over a frequency range.

A comparison is made between time domain data of shock pulses and frequency domain data derived from these pulses. The time domain data is used to get a peak ratio measurement, and is only one value of sensitivity for each shock pulse. Therefore, it is not a truly valid comparison to the frequency domain data, but should be close to those calculated values. This method of peak comparison in the time domain is widely used as a means for calibrating shock accelerometers, but does not provide any frequency or phase relationships since it only deals with peak amplitudes.

Discrete values of sensitivity, for peak comparison of the time domain data listed in table V, are plotted in figures 9a and 9c. Note that the abcissa, for the time domain values, is not labeled in terms of frequency. In the region from 500 to 2000 Hz, the sensitivity values from the time domain data, of the 500, 900, and 1500 g pulses, closely approximate the frequency domain sensitivities. This shows good agreement between the two methods. One exception from this correspondence is the time domain sensitivity for the 50 g pulse. In both accelerometers, A and B, this point is almost three percent lower than the other time domain values. At this time, this shift remains unexplained.

6.3.3 Intercomparisons Between Test Accelerometers. Phase and ratio data for this section are found in tables VII through XIV. Plots of the computed and measured ratio A/B can be found in figures 10a and 10c respectively. The major benefit of taking the computed ratio is that the errors due to the calibration factors of the reference accelerometer drop out. Thus, one source of error is eliminated. Phase relationships for the computed and measured ratios are plotted in figures 10e and 10g respectively. The standard deviations for these intercomparisons of the computed and measured ratios are plotted and shown in figures 10b, 10d, 10f, and 10h. The computed ratio of sinusoidal data are listed in table XII.

The ratio and phase relationships reveal that while the computed data are smooth curves with small standard deviations, the measured data ratios are erratic, but also have small standard deviations. This can be accounted for from the physical test conditions under which the two accelerometers, A and B, were tested in relation to each other. The measured data for this relationship were taken when the two pickups were mounted side-by-side, to the left and right of the center of the shock machine carriage. Therefore, any rocking motion would force one accelerometer to sense different motion from the other accelerometer. This difference would also introduce a false phase relationship. To lessen the errors in this kind of situation, pickups should be mounted as close to each other as possible.

7. CONCLUSIONS

7.1 General Overview and Summary

The results obtained from this project demonstrate that a fast, accurate method for shock calibration, by comparison methods, is feasible. The fast Fourier Transform algorithm makes this possible, because of its ability to handle large data blocks, its relative speed in analysis, and its accuracy. Use of a minicomputer, as a data collection device, provides a means to do preliminary processing and to transport the data to a larger computing machine via paper or magnetic tape. Shock calibrations in the frequency domain agreed to about one percent of the sinusoidal calibrations on each of the two accelerometers tested. Time domain, peak amplitude ratio calibrations agreed to about five percent of the sinusoidal calibration, depending on what frequency is selected. Frequency domain calibrations become unreliable when the Fourier amplitudes at high frequencies become less than a few percent of the low frequency amplitude.

For the 50 g, 8.5 ms shock pulses, calibration was reliable from 50 to about 300 Hz. For the 500 g, 1.2 ms and 900 g, 1.0 ms pulses, calibration was reliable from 50 Hz to about 2000 Hz. For the 1500 g, 0.7 ms pulse, the calibration appeared reliable from about 300 Hz to 4000 Hz or more; the analysis was not extended beyond 4000 Hz.

7.2 Future Considerations

Because the results obtained from the NBS developed shock calibration facility are favorable, further improvements are anticipated to account for any of the small problems encountered. These can include: (1) experimentation on the mounting locations of an accelerometer on the shock machine carriage, (2) implementation of a faster, more accurate FFT algorithm, (3) use of higher frequency content and amplitude pulses, (4) minimization of errors introduced by discontinuous data or data having steps, and (5) use of an algorithm which generates a finer frequency resolution (i.e, smaller Δf) for low frequencies.

A system incorporating a laser interferometer to measure instantaneous velocity is being developed. This interferometer system can, in principle, provide an absolute calibration facility for measuring shock induced motion.

8. ACKNOWLEDGMENTS

The authors wish to thank the following members of the Vibration Section for their aid and support in the development and assistance on the experimental work: Robert S. Koyanagi, James D. Pollard and Oliver W. Price. B. F. Payne is credited with the preliminary programming of the minicomputer. Thanks are due William H. Walston, Jr. for his assistance in the final stages of this work. Lowell D. Ballard and William Epstein are acknowledged as the original workers on this project and were responsible for most of the hardware and many of the initial concepts of shock calibration by use of Fourier analysis.

This paper reflects several stimulating and helpful discussions with Hans J. Oser, Walter L. Sadowski, and Daniel W. Lozier of the Mathematical Analysis Section. Acknowledgements are also due Richard N. Freemire for his magnetic tape reading routine and programming assistance.

9. REFERENCES

1. AVCO Technical Manual RAD-DM-STM51-1, AVCO Electronics Division, Tulsa Operation, Tulsa, Oklahoma.

2. American National Standard, "Methods for Specifying the Performance of Shock Machines", ANSI S2.14-1973.

3. Military Standard, "Environmental Test Methods", MIL-STD-810B, Method 516, 1967.

4. Military Standard, "Test Methods for Electronic and Electrical Component Parts", MIL-STD-202C, Method 213, 1963 (new method 213 added by change notice 2, May 1965).

5. Payne, B. F., "Absolute Calibration of Vibration Generators with Time-Sharing Computer as an Integral Part of System", Shock and Vibration Bulletin No. 36, Part 6, February 1967, pp.193-194.

6. Payne, B. F., "An Automated Precision Calibration System for Accelerometers", Instrument Society of America 17th National Aerospace Instrumentation Symposium, May 10-12, 1971 (Las Vegas, Nevada).

7. Dimoff, T., "Electrodynamic Vibration Standard With A Ceramic Moving Element", Journal of the Acoustical Society of America, Vol. 40, No. 3, September 1966, pp. 671-676.

8. Jones, E., Yelon, W. B., and Edelman, S., "Piezoelectric Shakers for Wide-Frequency Calibration of Vibration Pickups", Journal of the Acoustical Society of America, Vol. 45, No. 6, June 1969, pp. 1556-1559.

9. Schmidt, V. A., Edelman, S., Smith E. R., and Pierce, E. T., "Modulated Photoelectric Measurement of Vibration", Journal of Acoustical Society of America, Vol. 34, No. 4, April 1962, pp. 455-458.

10. Bouche, R. R., "Ensuring the Accuracy of Shock and Vibration Measurements", Proceeding of the Institute of Environmental Sciences, 1965, pp. 409-415. (Also reprinted by the Endevco Corporation as Publication TP 231.)

11. Bouche, R. R., "Accurate Accelerometer Calibrations by Absolute and Comparison Methods", Endevco Tech-Data Publication TP 233, March 1966.

12. Bouche, R. R., "Vibration Standards for Performing Comparison Calibrations", ISA reprint No. M18-3-MESTIND-67, 1967. (Also reprinted by the Endevco Corporation as Publication TP 241.)

13. Kistler, W. P., "New Precision Calibration Techniques for Vibration Transducers", Shock and Vibration Bulletin No. 35, Part 4, pp. 49-54, January 1966.

14. Bouche, R. R., Anspach, R. B., "Comparison Shock Motion Calibrations", 1968 Proceedings of the Institute of Environmental Sciences, (Also reprinted by the Endevco Corporation as Publication TP 240.)

15. Cooley, J. W. and Tukey, J. W., "An Algorithm for the Machine Calculation of Complex Fourier Series", Mathematics of Computers, Vol. 19, April 1965, pp. 297-301.

16. Peterson, A. P. G., and Gross, E. E., Handbook of Noise Measurements, General Radio Company, Concord, Massachusettes, 1972.

17. Bendat, J. S. and Piersol, A. G., Random Data: Analysis and Measurement Procedures, Wiley-Interscience, New York, 1972, pp. 233.

10. BIBLIOGRAPHY

1. Favour, J., "Transient Data Distortion Compensation", Shock and Vibration Bulletin 35, Part 5, pp. 231-238, February 1966.

2. Galef, A. E. and Mitchell, D. H., "Aerospace Industry Applications of the Fast Fourier Transform", Presented at Meeting of the Acoustical Society of America, Boston, Massachusetts, April 1973.

3. Favour, J. D., "Calibration of Accelerometers by Impulse Excitation and Fourier Transform Techniques", ISA Reprint Number P13-1-PHYMMID-67, 1967.

4. Bracewell, R., The Fourier Transform and Its Applications, McGraw-Hill, New York, 1965.

5. Hamming, R. W., Numerical Analysis for Scientists and Engineers, McGraw-Hill, New York, 1962.

6. American National Standard, "Acoustical Terminology (Including Mechanical Shock and Vibration)", ANSI S1.1-1960.

7. American National Standard, Methods for the Calibration of Shock and Vibration Pickups", ANSI S2.2-1959.

8. American National Standard, "Specifying the Characteristics of Auxiliary Equipment for Shock and Vibration Measurements", ANSI S2.4-1960.

9. American National Standard, "Selection of Calibrations and Tests for Electrical Transducers used for Measuring Shock and Vibration", ANSI S2.11-1969.

10. American National Standard, "Specifications for the Design, Construction, and Operation of Clash HI (High Impact) Shock Testing Machine for Lightweight Equipment", ANSI S2.15-1972.

TABLE I. Laboratory Test Matrix

Nominal Shock Pulse Parameters	Accelerometer Combinations[a]	Test Numbers
50 g, 8.5 ms	A/R	1-5
	B/R	6-10
	A/B	11-15
500 g, 1.2 ms	A/R	16-20
	B/R	21-25
	A/B	26-30
900 g, 1.0 ms	A/R	31-35
	B/R	36-40
	A/B	41-45
1500 g, 0.7 ms	A/R	46-50
	B/R	51-55
	A/B	56-60

[a]See Section 2 and 4.4 for description of accelerometers.

TABLE II. Acceleration Amplitudes and Durations.

Nominal Shock Pulse Parameters	Mean Amplitude	Amplitude Range	Measured from Test Numbers
50 g, 8.5 ms	52.4 g	49.4-55.8 g	1-10
500 g, 1.2 ms	517.5 g	488-560 g	16-25
900 g, 1.0 ms	894 g	864-927 g	31-40
1500 g, 0.7 ms	1419 g	1346-1524 g	46-54

TABLE III. Weighting Factors for the Calculations of Weighted Means of Accelerometers A and B. Data from Sinusoidal Calibrations.

Frequency Interval Hz	System and Date								
	D201/203 Dec 1972		D102 Dec 1972		D201 Apr 1970		D102 Apr 1970		Inter-ferometer Apr 1970
	Run 1	Run 2	Run 1	Run 2	Run 1	Run 2	Run 1	Run 2	
	Weighting Factors[a]								
10-900	2	2	2	2	1	1	1	1	0
1000-2500	2	2	2	2	1	1	1	1	4
3000-4000	2	2	2	2	1	1	0	0	4
4500-10,000	2	2	0	0	1	1	0	0	8

[a] No date was available in regions where a zero is indicated.

TABLE IV. Results of Sinusoidal Calibration of Accelerometers A, B, and R. Values given for A and B are in units of pC/g and values for R are units of mV/g.

Frequency Hz	Accelerometer A Sens.			Accelerometer B Sens.			Accelerometer R Sens.[a]		
	Wt'd. Mean	Fit Value	% Diff.	Wt'd. Mean	Fit Value	% Diff.	Wt'd. Mean	Fit Value	% Diff.
10	0.870	----	----	0.848	----	----	----	----	----
15	0.857	----	----	0.834	----	----	----	----	----
30	0.840	----	----	0.826	----	----	9.99	9.97	+0.2
50	0.842	0.846	-0.5	0.819	0.823	-0.5	9.98	9.97	+0.1
100	0.834	0.839	-0.6	0.811	0.817	-0.7	9.96	9.97	-0.1
200	0.830	0.833	-0.3	0.808	0.811	-0.3	9.95	9.97	-0.2
300	0.830	0.829	+0.1	0.806	0.807	-0.2	9.94	9.97	-0.3
400	0.826	0.826	-0.1	0.803	0.805	-0.2	9.96	9.97	-0.1
500	0.823	0.824	-0.2	0.801	0.803	-0.2	9.97	9.97	0.0
600	0.822	0.823	-0.1	0.800	0.801	-0.2	9.97	9.97	0.0
700	0.820	0.821	-0.1	0.799	0.800	-0.2	9.97	9.97	0.0
800	0.819	0.820	-0.1	0.798	0.799	-0.2	9.97	9.97	0.0
900	0.819	0.819	0.0	0.797	0.798	-0.1	9.98	9.97	+0.1
1000	0.819	0.818	+0.1	0.799	0.797	+0.3	9.99	9.98	+0.1
1500	0.816	0.815	+0.2	0.795	0.793	+0.2	9.99	9.98	+0.1
1700	0.815	----	----	0.794	----	----	9.99	9.98	+0.1
2000	0.813	0.814	-0.1	0.794	0.793	+0.1	9.99	9.98	+0.1
2500	0.812	0.814	-0.2	0.793	0.793	0.0	9.98	9.98	0.0
3000	0.814	0.814	0.0	0.792	0.794	-0.2	9.98	9.98	0.0
3500	0.815	0.814	+0.1	0.793	0.794	-0.2	9.97	9.98	-0.1
4000	0.814	0.814	0.0	0.794	0.795	-0.1	9.97	9.98	-0.1
4500	0.814	0.814	0.0	0.795	0.795	0.0	9.97	9.99	-0.2
5000	0.814	0.814	0.0	0.798	0.796	+0.3	10.09	10.03	+0.6
5500	0.819	----	----	0.800	----	----	10.06	10.07	-0.1
6000	0.828	0.824	+0.4	0.803	0.806	-0.4	10.07	10.11	-0.4
6500	0.827	----	----	0.816	----	----	10.07	10.14	-0.7
7000	0.832	0.832	-0.1	0.814	0.814	-0.1	10.15	10.17	-0.2
7500	0.833	----	----	0.818	----	----	10.19	10.20	-0.1
8000	0.844	0.840	+0.5	0.822	0.822	0.0	10.22	10.23	-0.1
8500	0.846	----	----	0.827	----	----	10.25	10.25	0.0
9000	0.848	0.846	+0.2	0.827	0.828	-0.1	10.30	10.27	+0.3
9500	0.852	----	----	0.834	----	----	10.34	10.30	+0.4
10000	0.853	0.852	+0.1	0.836	0.834	+0.2	10.32	10.32	0.0

[a]Amplifier was at nominal setting of 10 mV/g and the filter out. For sensitivities at a setting of 1 mV/g, divide fit values by 10.

TABLE V. Peak Comparison Calibrations of Accelerometers A and B.

Nominal Impact Parameter	Accelerometer Sensitivity, pC/g				Sensitivity Ratios, A/B			
	Accelerometer A		Accelerometer B		Measured		Calculated	
	Sens.[a]	% Std. Dev.	Sens.[a]	% Std. Dev.	Ratio	% Std. Dev.	Ratio[c]	% Std. Dev.[d]
50 g, 8.5 ms	0.7894	0.1	0.7750	0.7	1.0261	0.1	1.0186	1.3
500 g, 1.2 ms	0.8125	0.1	0.7947	0.2	1.0069[b]	0.3	1.0224	0.2
900 g, 1.0 ms	0.8180	0.2	0.7930	0.2	0.9539[b]	0.1	1.0315	0.3
1500 g, 0.7 ms	0.8135	0.1	0.7955	0.9	0.9049[b]	0.2	1.0226	0.9
Group Mean	0.8147[e]	0.1[f]	0.7896[e]	0.6[f]	0.9730[b,e]	0.2[f]	1.0238[e]	0.8[f]

[a] A system sensitivity of accelerometer R at 100 Hz of S_r = 9.969 mV/g was used for these calculations.

[b] Low pass filters were used to improve time-domain wave shapes for indicated measurements. It is not possible to correct for the filter effects.

[c] Calculated from columns 2 and 4 of this table.

[d] Calculated from columns 3 and 5 of this table on root-sum-squared basis.

[e] Column means.

[f] Group standard deviation calculated rms basis, i.e., $\sqrt{(\sigma_1^2 + \sigma_2^2 + \sigma_3^2 + \sigma_4^2)/4}$.

TABLE VI. Information for Averaging Over Frequency Ranges for Shock Data.

Frequency Range Hz	Plotting Interval	Data Points		Total No. of Measurement Results in Ave.
		Number of Points	Frequency Span, Hz	
$50 \leq f \leq 500$	50	1	f	5
$600 \leq f \leq 1000$	100	3	f±50	15
$1000 \leq f \leq 2000$	250	11	f±250	55
$2500 \leq f \leq 5000$	500	21	f±500	105
$6000 \leq f \leq 10000$	1000	41	f±1000	205

TABLE VII. Accelerometer A Sensitivity and Standard Deviation.

Frequency	50 g	σ_{50}	500 g	σ_{500}	900 g	σ_{900}	1500 g	σ_{1500}
Hz	pC/g	%	pC/g	%	pC/g	%	pC/g	%
50	.832	0.1	.846	0.3	.824	0.2	.885	2.1
100	.828	0.2	.828	0.4	.830	0.2	.827	1.1
150	.824	0.0	.826	0.5	.831	0.2	.852	1.3
200	.832	0.8	.822	0.6	.825	0.3	.827	2.0
250	.800	0.5	.821	0.2	.825	0.1	.822	1.6
300	.796	4.6	.819	0.2	.820	0.2	.817	1.6
350	.817	2.5	.816	0.2	.821	0.1	.830	2.2
400	.723	7.0	.814	0.2	.817	0.2	.812	0.6
450	.769	6.0	.817	0.3	.816	0.0	.819	1.9
500	.787	9.1	.814	0.3	.816	0.1	.820	1.3
600	----	----	.810	0.4	.814	0.2	.820	1.6
700	----	----	.809	0.5	.813	0.1	.820	1.0
800	----	----	.807	0.3	.812	0.1	.818	1.1
900	----	----	.806	1.0	.811	0.1	.816	1.4
1000	----	----	.805	1.2	.811	0.1	.817	1.2
1250	----	----	.807	0.8	.813	0.3	.816	1.4
1500	----	----	.810	1.5	.817	0.4	.813	1.7
1750	----	----	.810	1.8	.821	0.4	.813	1.8
2000	----	----	.811	2.4	.824	0.4	.809	1.5
2500	----	----	.808	4.9	.821	1.7	.816	1.3
3000	----	----	.819	10.6	.824	7.1	.821	1.5
3500	----	----	.824	13.3	.834	7.3	.826	1.7
4000	----	----	.905	63.5	.831	3.7	.829	1.5
4500	----	----	.827	90.0	.815	4.9	.840	1.6

TABLE VIII. Accelerometer B Sensitivity and Standard Deviation.

Frequency	50g	σ_{50}	500 g	σ_{500}	900 g	σ_{900}	1500 g	σ_{1500}
Hz	pC/g	%	pC/g	%	pC/g	%	pC/g	%
50	.805	0.1	.814	0.7	.819	0.3	.836	10.7
100	.800	0.1	.812	0.4	.808	0.2	.785	4.4
150	.797	0.2	.804	0.4	.806	0.2	.814	6.2
200	.800	0.4	.802	0.1	.806	0.2	.812	4.9
250	.789	0.6	.808	0.4	.803	0.1	.800	4.6
300	.791	1.5	.802	0.4	.802	0.2	.788	2.9
350	.754	1.6	.802	0.3	.800	0.4	.794	3.6
400	.781	7.0	.797	0.1	.800	0.3	.797	3.1
450	.712	5.6	.798	0.2	.797	0.2	.791	3.2
500	.741	5.9	.798	0.3	.796	0.3	.796	2.8
600	----	----	.793	0.3	.794	0.2	.793	3.1
700	----	----	.793	0.3	.793	0.3	.798	3.6
800	----	----	.791	0.2	.792	0.2	.793	3.4
900	----	----	.790	0.2	.791	0.2	.799	3.6
1000	----	----	.788	0.3	.791	0.1	.790	2.7
1250	----	----	.788	0.4	.794	0.6	.789	2.1
1500	----	----	.787	0.7	.797	0.8	.789	2.0
1750	----	----	.785	0.7	.797	0.7	.790	3.2
2000	----	----	.782	1.0	.794	0.5	.778	2.1
2500	----	----	.773	1.9	.798	1.2	.797	2.0
3000	----	----	.771	4.3	.803	1.8	.803	2.0
3500	----	----	.790	8.1	.809	2.2	.811	1.9
4000	----	----	.803	20.2	.826	3.6	.826	2.4
4500	----	----	.817	45.4	.880	7.4	.836	2.7

TABLE IX. Accelerometer A Phase and Standard Deviation in Degrees.

Frequency Hz	50 g	σ_{50}	500 g	σ_{500}	900 g	σ_{900}	1500 g	σ_{1500}
50	-0.8	0.0	-0.2	0.3	-0.7	0.2	-2.6	1.5
100	-0.7	0.1	-0.4	0.2	-0.8	0.1	-1.5	0.8
150	-0.7	0.1	-0.5	0.1	-1.0	0.1	-0.7	1.2
200	-0.4	0.5	-0.9	0.1	-1.0	0.1	-1.6	1.3
250	-1.0	0.6	-1.0	0.1	-1.2	0.1	-2.6	0.7
300	-1.2	0.7	-0.7	0.2	-1.3	0.2	-1.9	0.6
350	+0.3	1.4	-0.9	0.1	-1.3	0.1	-2.0	0.6
400	-1.0	5.3	-1.0	0.2	-1.3	0.1	-1.7	0.8
450	-0.4	2.4	-1.1	0.1	-1.5	0.2	-2.4	1.1
500	-1.3	1.2	-0.9	0.3	-1.4	0.1	-2.1	1.7
600	-1.6	4.2	-1.0	0.2	-1.4	0.1	-1.4	0.7
700	-2.7	3.9	-1.0	0.2	-1.5	0.2	-1.8	0.9
800	-1.3	5.3	-0.9	0.2	-1.4	0.2	-1.4	1.1
900	-3.3	7.6	-1.1	0.3	-1.6	0.2	-2.2	1.0
1000	----	----	-0.9	0.2	-1.5	0.2	-2.8	0.8
1250	----	----	-1.0	0.3	-1.5	0.2	-2.6	0.9
1500	----	----	-1.0	0.3	-1.9	0.3	-2.6	1.1
1750	----	----	-1.1	0.5	-2.4	0.3	-3.0	1.1
2000	----	----	-1.1	0.7	-2.5	0.3	-3.2	1.1
2500	----	----	-1.0	1.2	-3.1	2.0	-3.4	1.2
3000	----	----	+0.1	2.4	-3.7	1.1	-3.9	1.2
3500	----	----	-0.3	4.6	-4.1	1.0	-4.3	1.3
4000	----	----	-1.8	10.0	-4.2	1.3	-4.8	1.5
4500	----	----	----	----	-6.4	5.8	-6.3	1.7

TABLE X. Accelerometer B Phase and Standard Deviation in Degrees.

Frequency Hz	50 g	σ_{50}	500 g	σ_{500}	900 g	σ_{900}	1500 g	σ_{1500}
50	-1.1	0.1	-0.1	0.1	-0.7	0.2	-1.2	0.8
100	-0.7	0.1	-0.3	0.3	-0.5	0.2	-1.1	0.6
150	-1.0	0.1	-1.0	0.2	-1.3	0.0	-0.7	0.7
200	-0.6	0.2	-0.9	0.2	-1.1	0.1	-2.5	1.1
250	-3.0	0.6	-1.0	0.1	-1.2	0.1	-1.6	0.9
300	+0.7	1.4	-0.9	0.1	-1.3	0.0	-1.1	0.9
350	+0.3	1.5	-0.9	0.4	-1.4	0.0	-1.7	0.6
400	+0.1	1.3	-1.3	0.3	-1.3	0.0	-1.6	1.4
450	-3.9	2.1	-1.0	0.3	-1.5	0.1	-1.4	0.6
500	-1.9	6.7	-0.9	0.1	-1.4	0.1	-1.1	0.9
600	-1.9	2.0	-1.0	0.2	-1.4	0.0	-1.6	0.8
700	-2.5	5.1	-1.1	0.4	-1.5	0.1	-1.8	0.9
800	-2.6	3.2	-0.9	0.4	-1.5	0.1	-2.0	0.8
900	-2.0	5.5	-1.0	0.2	-1.7	0.1	-2.4	0.6
1000	----	----	-0.8	0.2	-1.6	0.1	-2.2	0.6
1250	----	----	-0.6	0.7	-1.6	0.1	-2.5	0.9
1500	----	----	-0.5	0.7	-1.8	0.2	-2.9	1.1
1750	----	----	-0.6	0.9	-2.1	0.2	-3.2	1.1
2000	----	----	-0.7	1.2	-2.6	0.4	-3.5	0.8
2500	----	----	-0.7	3.4	-3.7	1.2	-3.6	0.7
3000	----	----	-2.1	8.1	-3.7	3.9	-4.0	0.9
3500	----	----	----	----	-4.7	4.2	-4.8	1.0
4000	----	----	----	----	-5.8	2.3	-5.0	0.9
4500	----	----	----	----	-6.1	2.4	-5.0	0.8

TABLE XI. Derived Ratio of Shock Data: A/B (From Tables VII and VIII) and Standard Deviation.

Frequency	50 g	σ_{50}	500 g	σ_{500}	900 g	σ_{900}	1500 g	σ_{1500}
Hz	pC/g	%	pC/g	%	pC/g	%	pC/g	%
50	1.03	0.1	1.04	0.5	1.03	0.3	1.06	7.7
100	1.04	0.2	1.02	0.4	1.03	0.2	1.05	3.2
150	1.03	0.2	1.03	0.4	1.03	0.2	1.05	4.5
200	1.04	0.7	1.02	0.4	1.02	0.2	1.02	3.7
250	1.01	0.6	1.02	0.3	1.03	0.1	1.03	3.5
300	1.01	3.4	1.02	0.3	1.02	0.2	1.04	2.3
350	1.08	2.1	1.02	0.2	1.03	0.3	1.04	3.0
400	0.93	7.0	1.02	0.2	1.02	0.2	1.02	2.2
450	1.08	4.4	1.02	0.3	1.02	0.1	1.04	2.6
500	1.06	7.7	1.02	0.3	1.03	0.2	1.03	2.2
600	----	----	1.02	0.3	1.02	0.2	1.03	2.5
700	----	----	1.02	0.4	1.03	0.2	1.03	2.6
800	----	----	1.02	0.3	1.03	0.2	1.03	2.5
900	----	----	1.02	0.7	1.03	0.1	1.02	2.8
1000	----	----	1.02	0.8	1.03	0.1	1.03	2.1
1250	----	----	1.02	0.6	1.02	0.4	1.03	1.8
1500	----	----	1.03	1.2	1.02	0.6	1.03	1.9
1750	----	----	1.03	1.4	1.03	0.6	1.03	2.6
2000	----	----	1.04	1.8	1.04	0.5	1.04	1.8
2500	----	----	1.04	3.8	1.03	1.4	1.02	1.6
3000	----	----	1.06	8.1	1.03	5.2	1.02	1.8
3500	----	----	1.04	11.0	1.03	5.4	1.02	1.8
4000	----	----	1.13	47.1	1.01	3.7	1.00	2.0
4500	----	----	1.01	71.3	0.93	6.3	1.00	2.2

TABLE XII. Measured Ratio A/B of Shock and Sinusoidal Data with Standard Deviation.

Frequency	50 g	σ_{50}	500 g	σ_{500}	900 g	σ_{900}	1500 g	σ_{1500}	Sine
Hz		%		%		%		%	
50	1.00	0.2	0.99	0.4	1.01	0.1	1.10	0.8	1.03
100	1.03	0.2	1.02	0.0	0.97	0.5	1.05	1.1	1.03
150	0.98	3.0	1.08	0.3	1.10	0.2	1.16	1.0	1.03
200	1.04	6.7	1.06	0.4	1.09	0.1	1.07	0.3	1.03
250	1.20	15.3	1.04	0.2	1.07	0.2	1.19	1.5	1.03
300	0.65	37.2	1.05	0.4	1.02	0.1	1.05	0.6	1.03
350	----	----	1.03	0.4	1.03	0.2	1.12	1.0	1.03
400	----	----	1.04	0.4	1.08	0.1	1.08	1.2	1.03
450	----	----	1.03	0.3	1.06	0.2	1.09	0.7	1.03
500	----	----	1.05	0.6	1.02	0.6	1.12	0.9	1.03
600	----	----	1.02	0.7	1.06	0.8	1.11	0.7	1.03
700	----	----	1.02	0.6	1.05	0.8	1.11	0.6	1.03
800	----	----	1.02	0.5	1.08	1.2	1.12	0.7	1.03
900	----	----	1.02	0.5	1.07	0.5	1.12	0.8	1.03
1000	----	----	1.02	0.4	1.10	0.7	1.12	0.9	1.03
1250	----	----	1.02	0.4	1.12	1.0	1.14	1.0	1.03
1500	----	----	1.02	0.5	1.15	1.3	1.15	1.1	1.03
1750	----	----	1.02	0.8	1.20	1.7	1.16	1.1	1.03
2000	----	----	1.03	0.8	1.28	3.3	1.17	1.1	1.03
2500	----	----	1.06	2.6	1.57	9.8	1.20	1.3	1.03
3000	----	----	1.14	5.7	----	----	1.23	1.7	1.03
3500	----	----	1.35	14.3	----	----	1.26	2.1	1.02
4000	----	----	----	----	----	----	1.31	2.4	1.02
4500	----	----	----	----	----	----	1.36	2.9	1.02
5000	----	----	----	----	----	----	----	----	1.02
6000	----	----	----	----	----	----	----	----	1.02
7000	----	----	----	----	----	----	----	----	1.02
8000	----	----	----	----	----	----	----	----	1.02
9000	----	----	----	----	----	----	----	----	1.02
10000	----	----	----	----	----	----	----	----	1.02

TABLE XIII. Computed Phase Difference: A/B (From Tables IX and X) and Standard Deviation in Degrees.

Frequency Hz	50 g	σ_{50}	500 g	σ_{500}	900 g	σ_{900}	1500 g	σ_{1500}
50	-0.3	0.1	+0.1	0.3	-0.0	0.2	+1.4	1.2
100	-0.0	0.1	+0.1	0.2	+0.4	0.1	+0.4	0.7
150	-0.3	0.1	-0.5	0.2	-0.4	0.1	-0.0	1.0
200	-0.2	0.4	-0.0	0.2	-0.1	0.1	-0.9	1.2
250	-2.0	0.6	+0.0	0.1	-0.0	0.1	+1.0	0.8
300	+1.9	1.1	-0.1	0.2	-0.0	0.1	+0.8	0.8
350	+0.0	1.5	+0.0	0.3	-0.1	0.1	+0.2	0.6
400	+1.1	3.9	-0.3	0.3	+0.0	0.1	+0.0	1.1
450	-3.5	2.2	+0.0	0.2	+0.0	0.1	+1.0	0.9
500	-0.6	4.8	-0.0	0.2	-0.1	0.1	+1.0	1.4
600	-0.3	3.3	-0.0	0.2	+0.0	0.1	-0.2	0.8
700	+0.2	4.5	-0.1	0.3	-0.0	0.1	-0.1	0.9
800	-1.3	4.4	+0.0	0.3	-0.1	0.1	-0.7	0.9
900	+1.3	6.6	+0.1	0.2	-0.1	0.2	-0.2	0.8
1000	----	----	+0.1	0.2	-0.1	0.2	+0.5	0.7
1250	----	----	+0.4	0.5	-0.1	0.3	+0.1	0.9
1500	----	----	+0.5	0.6	-0.1	0.2	-0.3	1.1
1750	----	----	+0.5	0.7	+0.3	0.3	-0.2	1.1
2000	----	----	+0.4	0.9	-0.1	0.4	-0.2	1.0
2500	----	----	+0.3	2.6	-0.6	1.6	-0.2	1.0
3000	----	----	-2.2	6.0	-0.1	2.9	-0.1	1.0
3500	----	----	----	----	-0.6	3.0	-0.5	1.1
4000	----	----	----	----	-1.6	1.8	-0.2	1.2
4500	----	----	----	----	+0.3	4.4	+1.4	1.3

TABLE XIV. Phase Difference from Measured Ratio A/B and Standard Deviation in Degrees.

Frequency Hz	50 g	σ_{50}	500 g	σ_{500}	900 g	σ_{900}	1500 g	σ_{1500}
50	+2.5	0.0	-0.2	0.7	-0.7	0.1	+4.7	0.6
100	+0.5	0.1	+3.7	1.5	+4.1	0.2	+4.6	0.7
150	+1.7	0.3	+1.2	0.1	+3.7	0.2	+3.1	0.6
200	+15.3	1.4	+0.4	0.3	+0.7	0.2	+1.3	0.7
250	-73.7	11.8	-1.4	0.5	-1.6	0.1	+1.9	0.2
300	+34.9	115.7	-0.0	0.9	-0.5	0.2	-2.9	0.4
350	+33.6	73.4	-1.1	0.5	+2.1	0.3	+3.2	0.9
400	----	----	-0.3	0.9	+1.0	0.3	-1.6	0.3
450	----	----	-0.7	0.9	-0.9	0.6	+3.3	0.5
500	----	----	-1.1	1.2	+0.2	0.3	+0.3	0.5
600	----	----	-1.0	1.3	+0.8	0.7	+0.9	0.6
700	----	----	-1.0	1.4	+1.1	0.7	+1.1	0.5
800	----	----	-0.9	1.7	+1.5	0.9	+1.5	0.6
900	----	----	-1.0	2.0	+1.3	0.8	+1.4	0.6
1000	----	----	-1.0	2.2	+1.5	1.1	+1.3	0.5
1250	----	----	-1.0	2.3	+1.6	1.5	+1.0	0.5
1500	----	----	-0.9	3.6	+2.2	1.9	+0.7	0.5
1750	----	----	-0.6	4.4	+3.0	2.5	-0.5	0.6
2000	----	----	-0.0	5.3	+3.7	3.1	-0.1	0.7
2500	----	----	+2.4	8.1	+4.5	3.8	-0.5	0.8
3000	----	----	+7.5	12.2	+0.9	4.7	-0.6	1.0
3500	----	----	+19.2	21.7	-15.2	11.8	-1.8	1.1
4000	----	----	----	----	-40.8	15.6	-2.3	1.5
4500	----	----	----	----	-61.1	14.1	-2.9	1.6

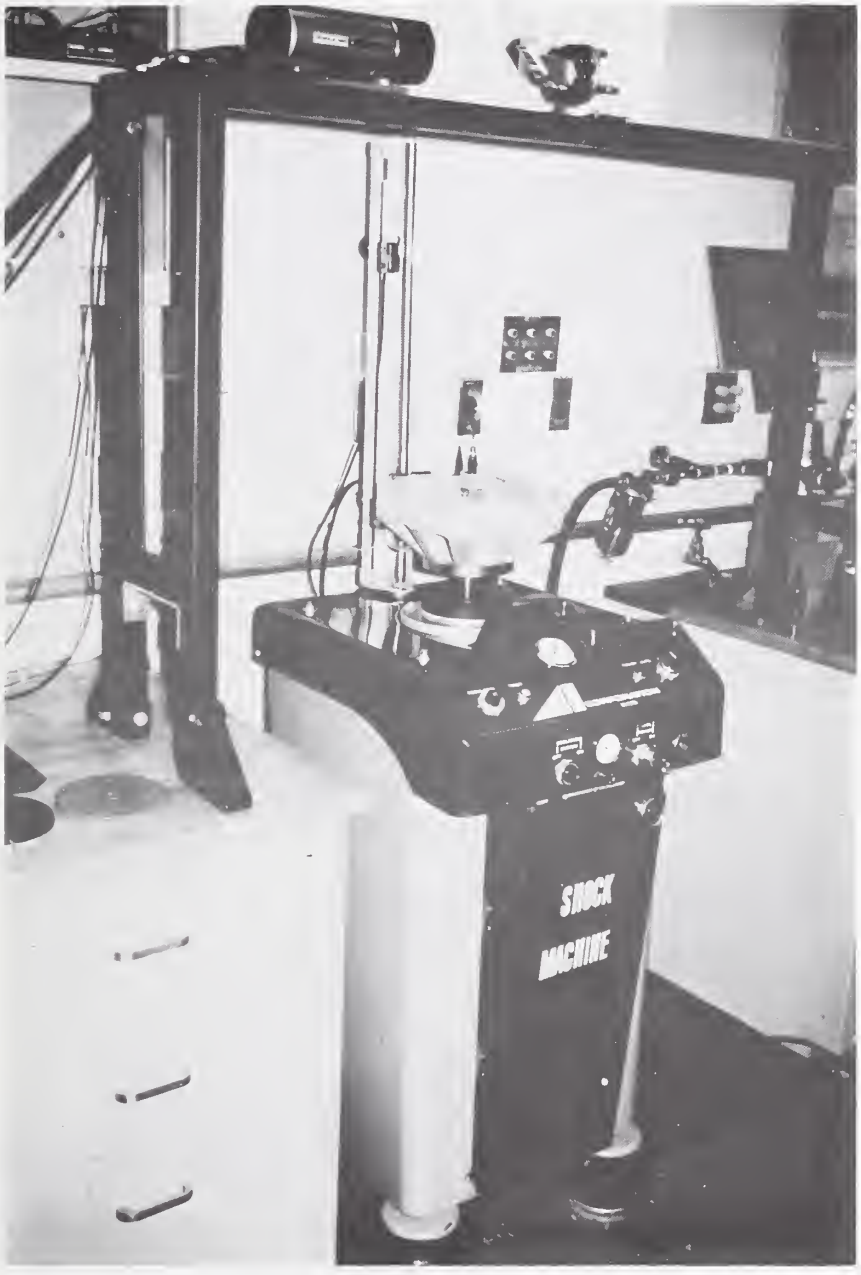

FIGURE 1. Mechanical Shock Generating Machine.

FIGURE 2. Typical Impact Pulses from Accelerometer B.

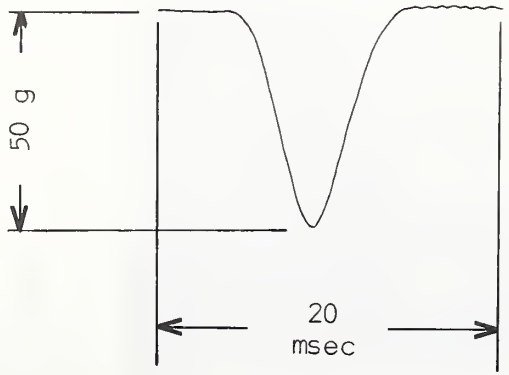

a. Test Number 4.

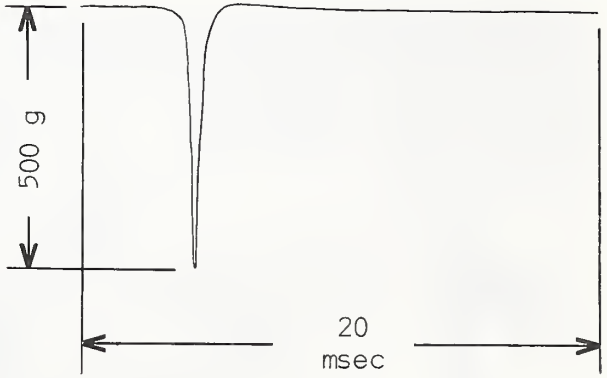

b. Test Number 16.

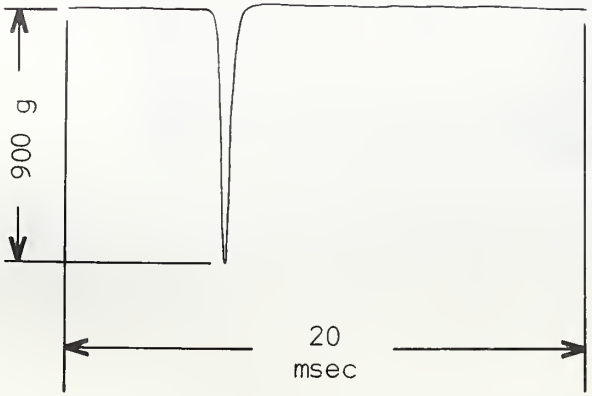

c. Test Number 31.

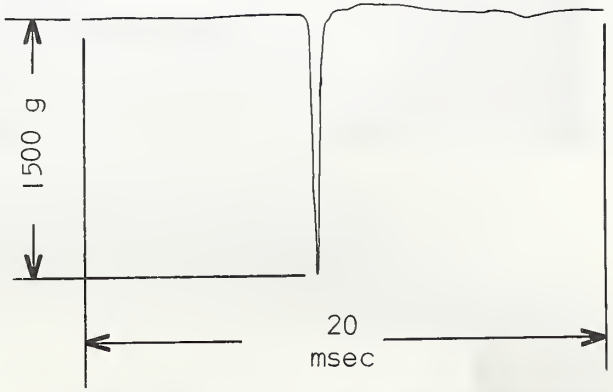

d. Test Number 46.

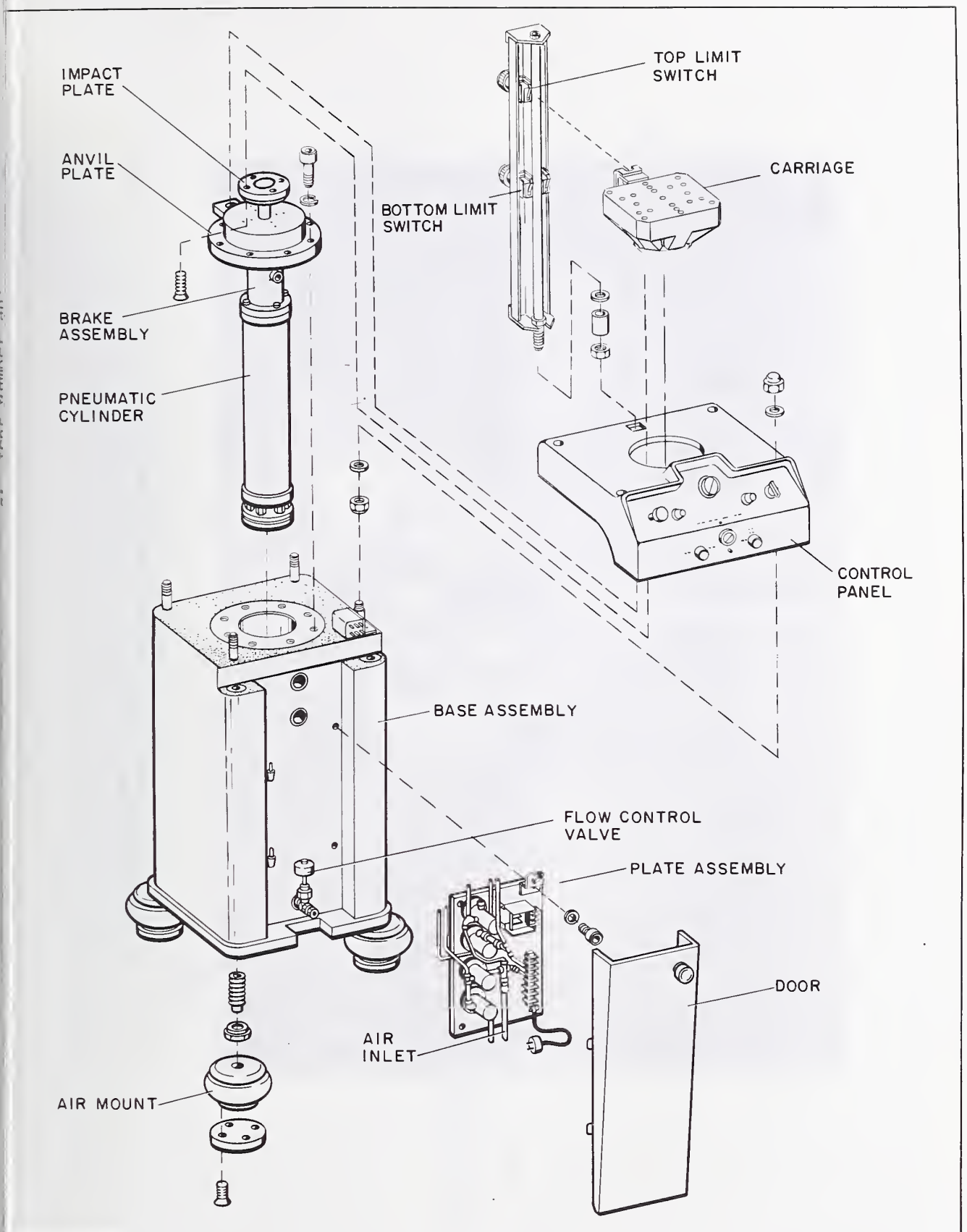

FIGURE 3. Exploded View of Shock Test Machine

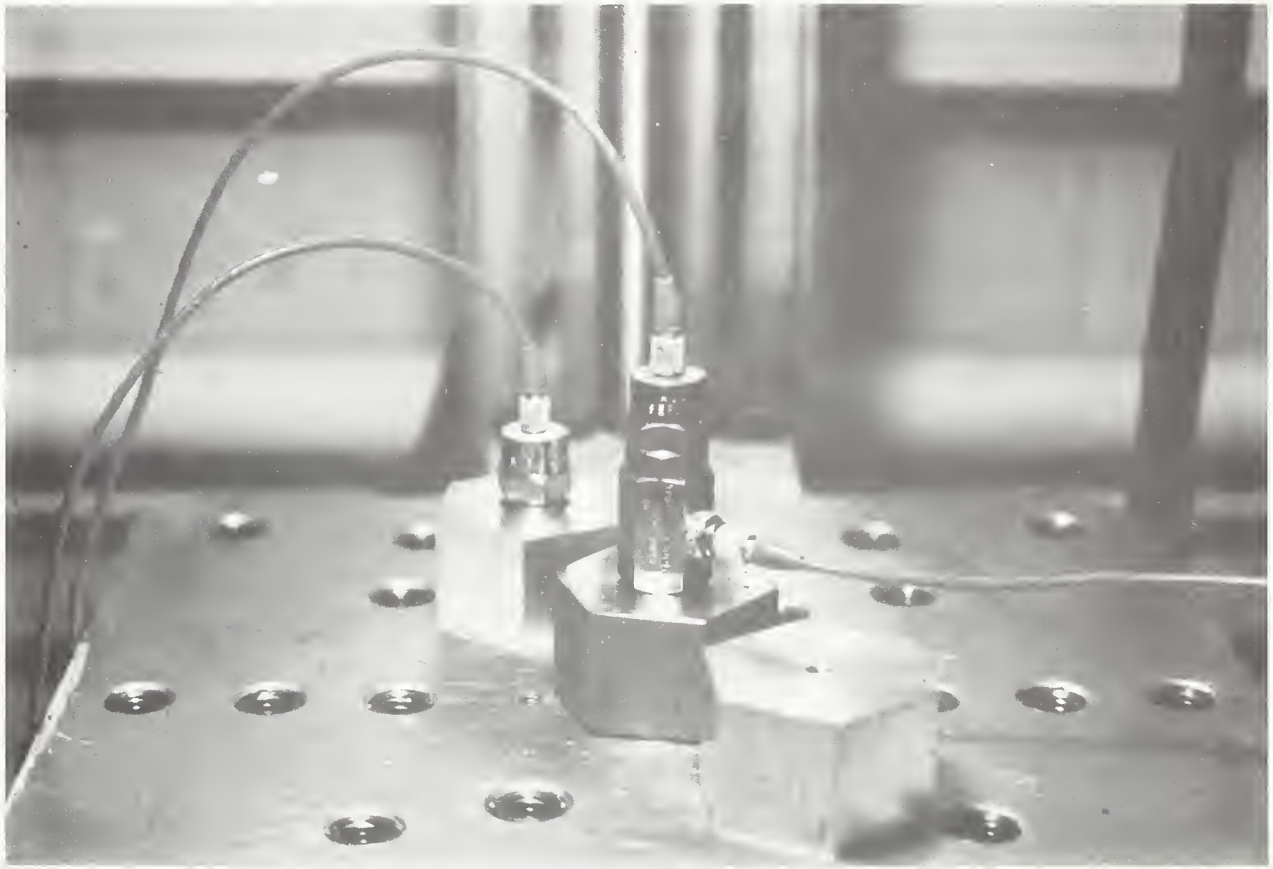

FIGURE 4. "Piggy-Back" Configuration of Reference Standard and Test Accelerometers, with Single Test Accelerometer Mounted Behind.

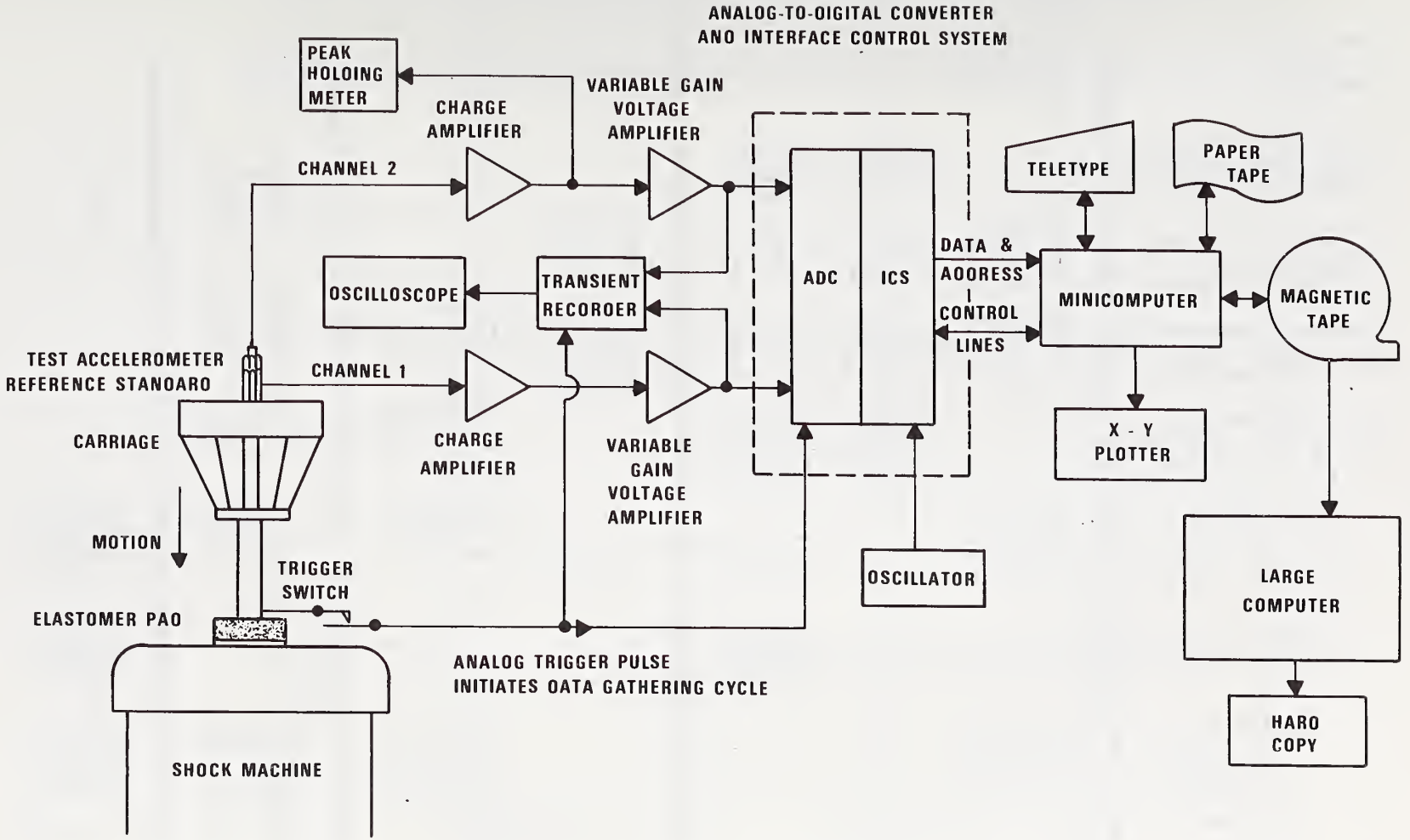

FIGURE 5. Block Diagram of Shock Pulse Data Generation, Retrieval, and Analysis.

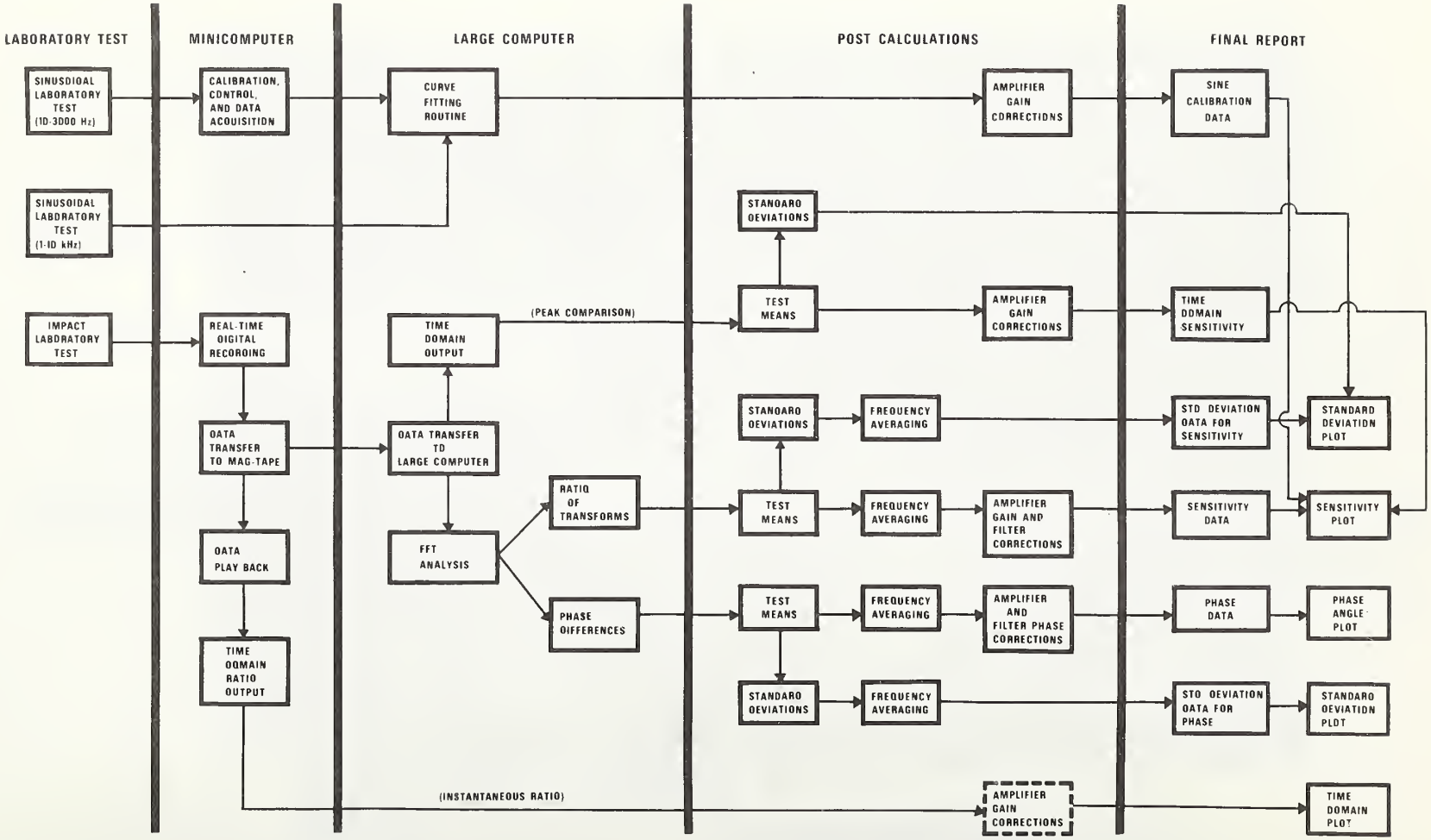

FIGURE 6. Data Processing and Analysis Steps for Sinusoidal and Shock Calibrations

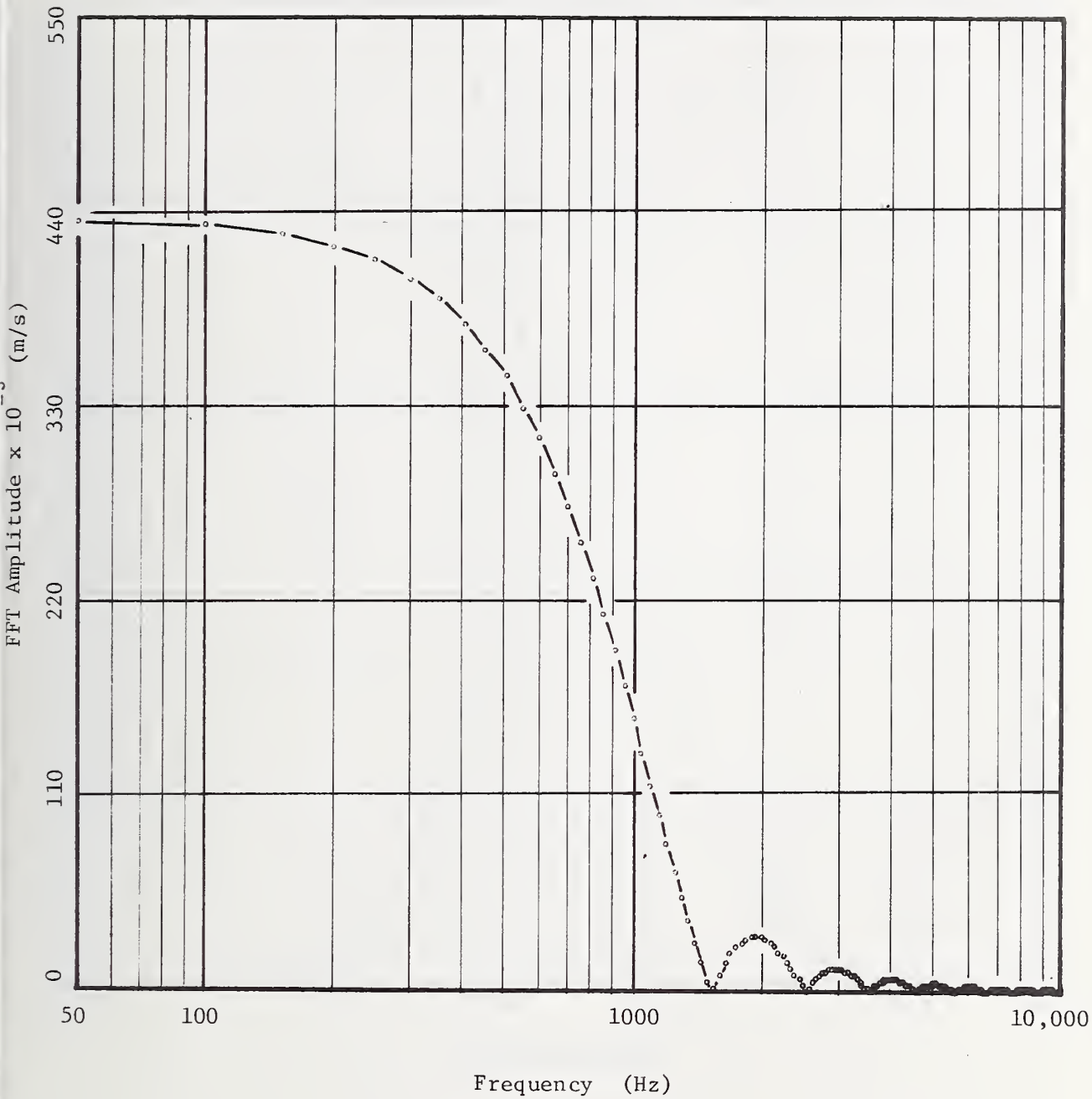

FIGURE 7a. Transform of 900 g Half-Sine Pulse.

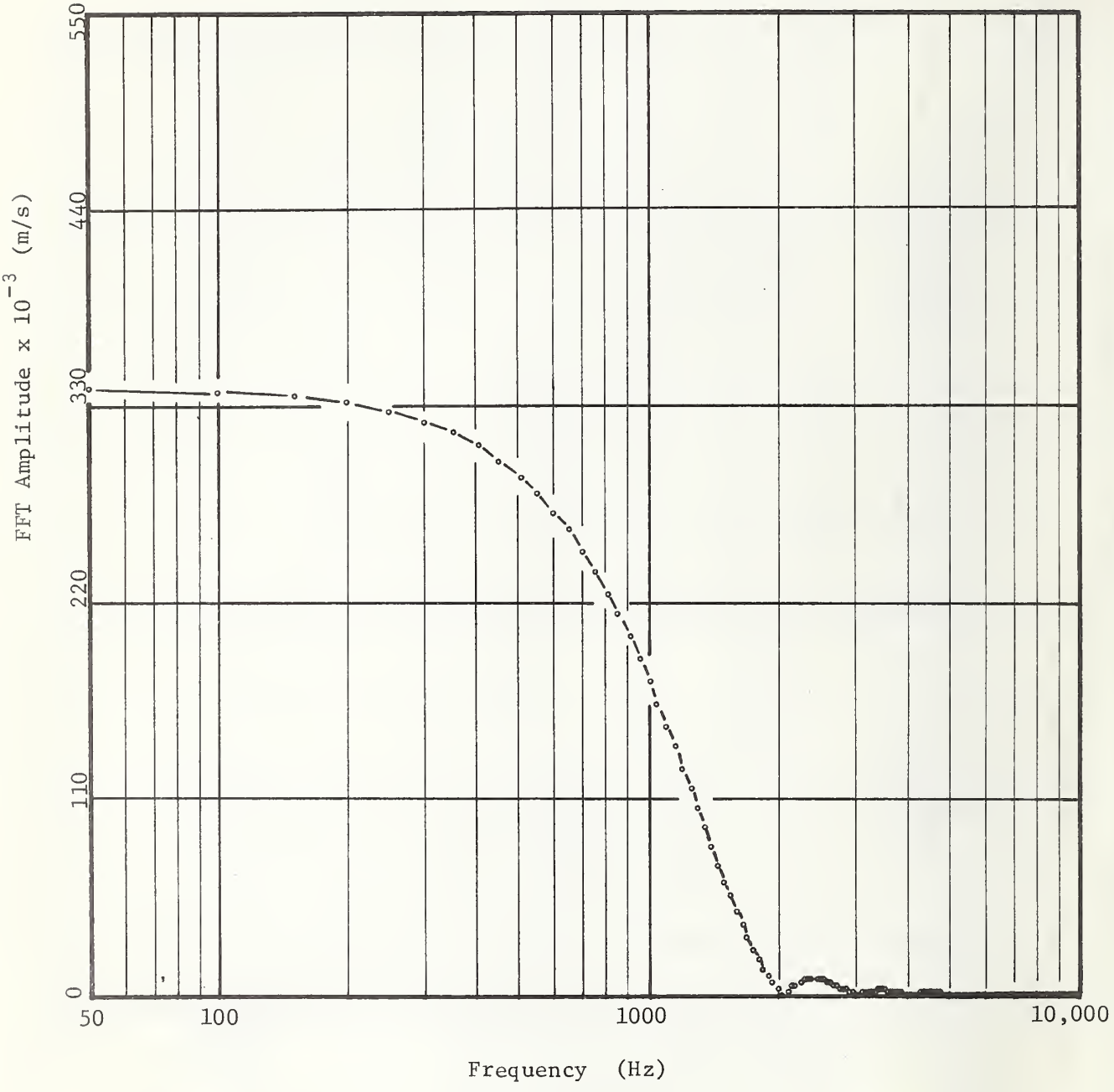

FIGURE 7b. Transform of 900 g Haversine Pulse.

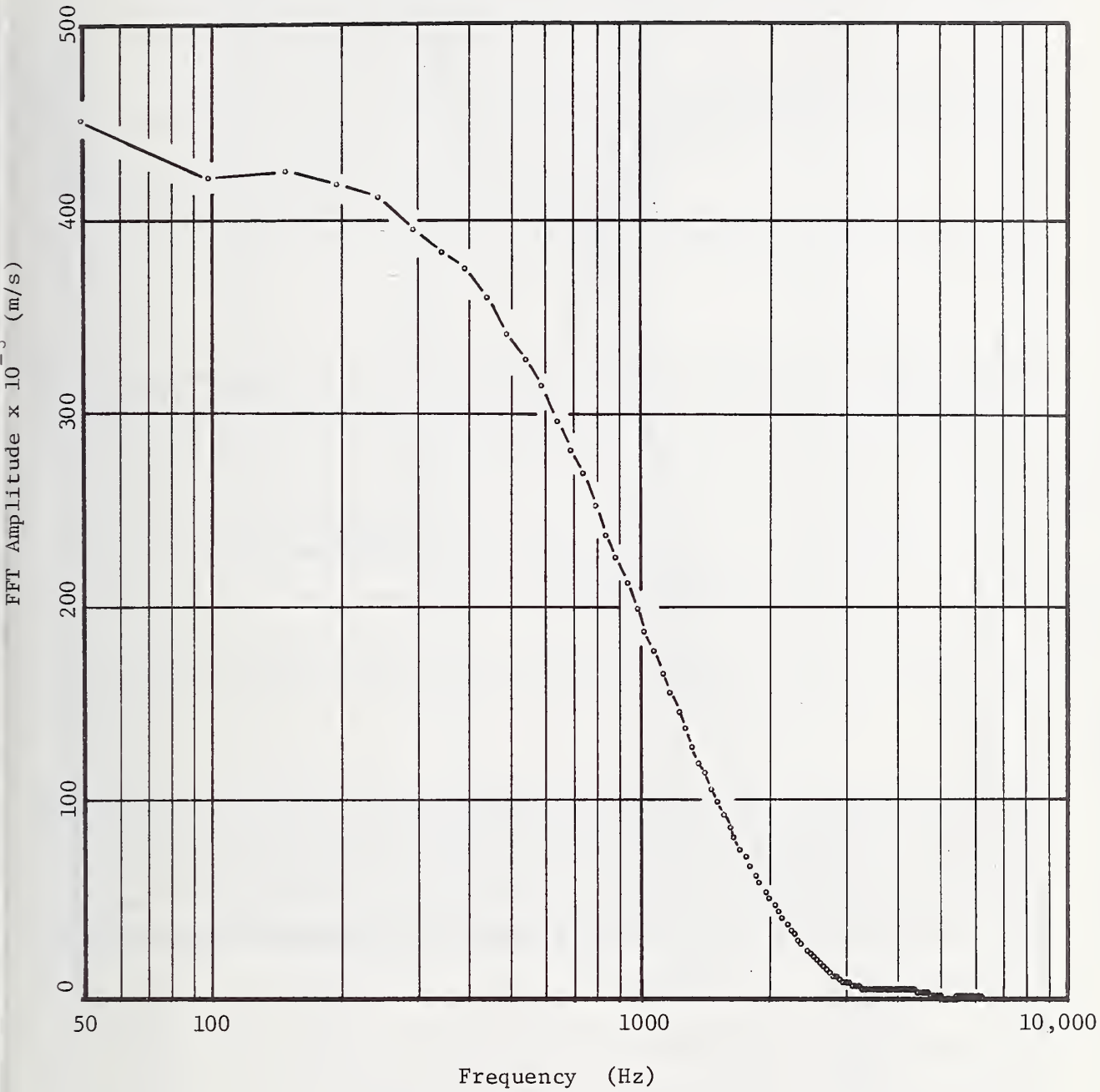

FIGURE 8. Transform of Actual 900 g Shock Pulse.

FIGURE 9a. Pickup A Sensitivity.

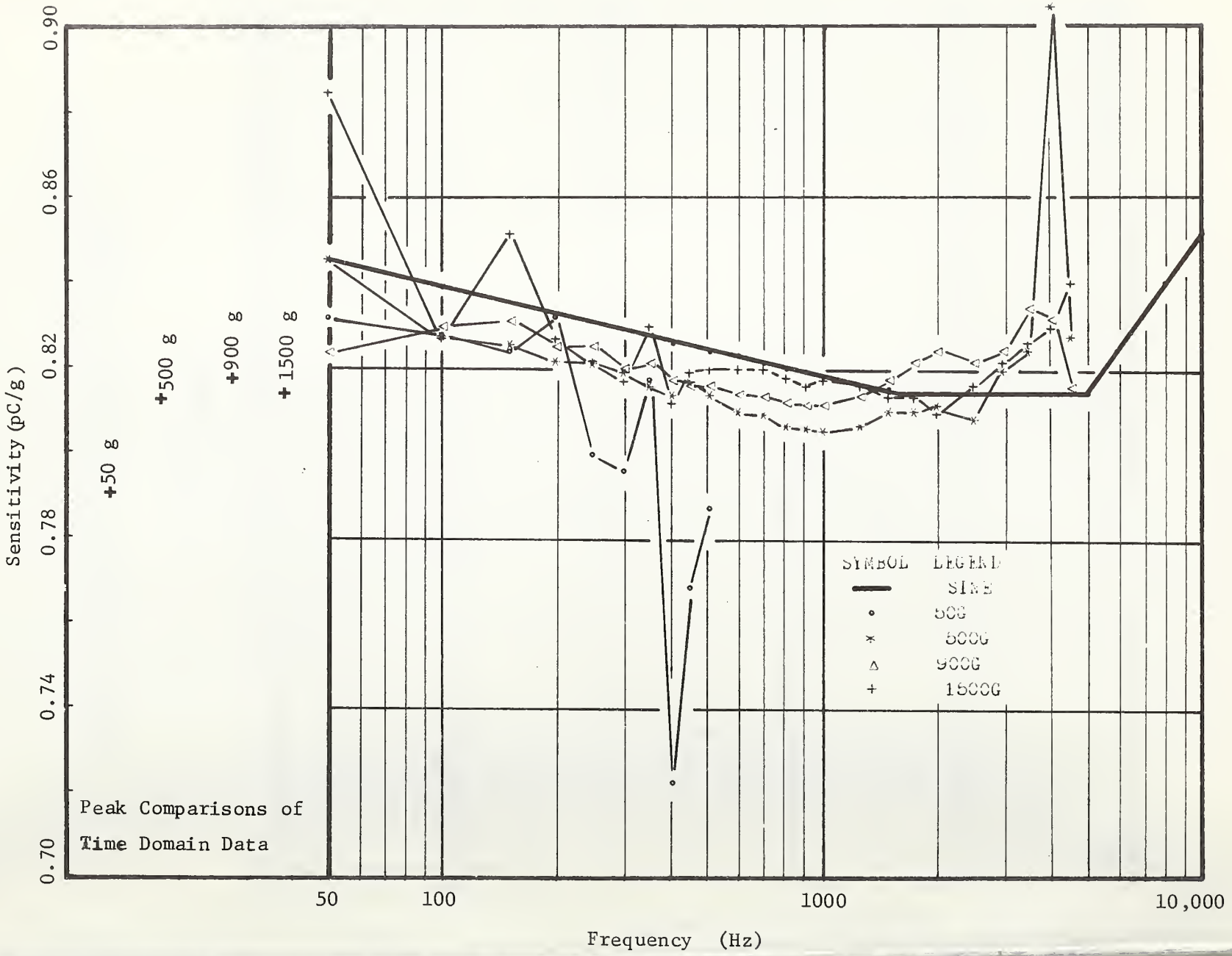

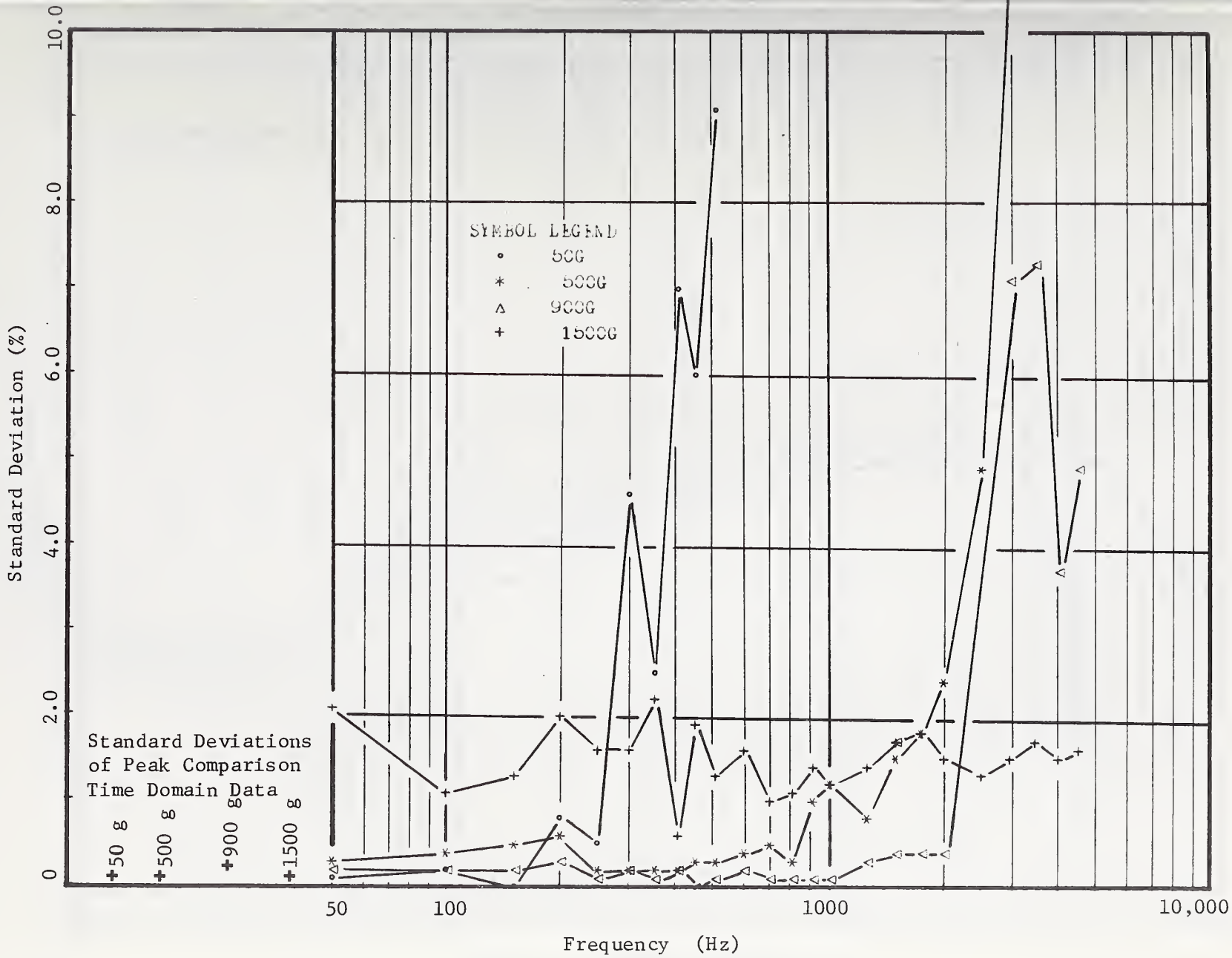

FIGURE 9b. Standard Deviations of Pickup A Sensitivities.

FIGURE 9c. Pickup B Sensitivity.

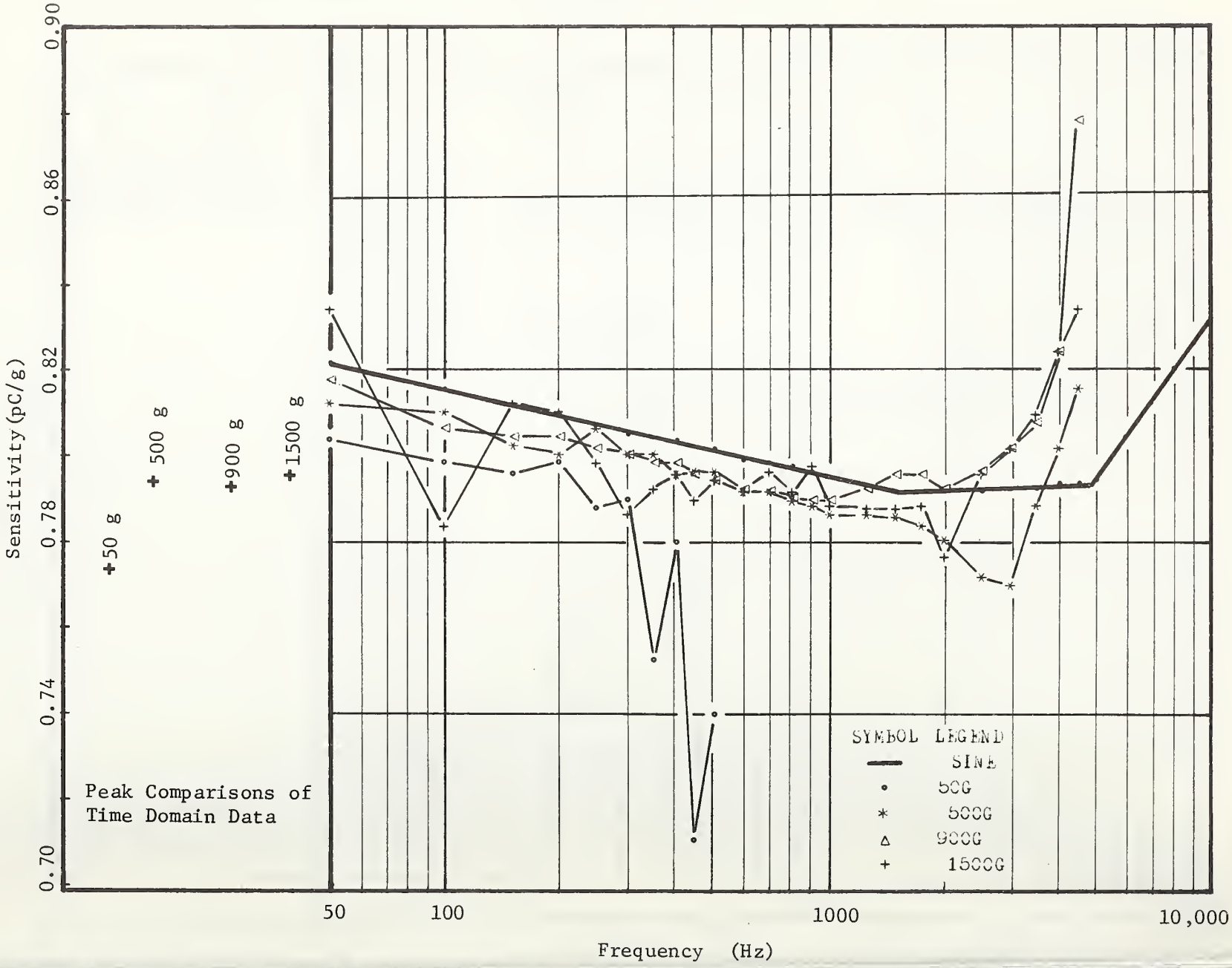

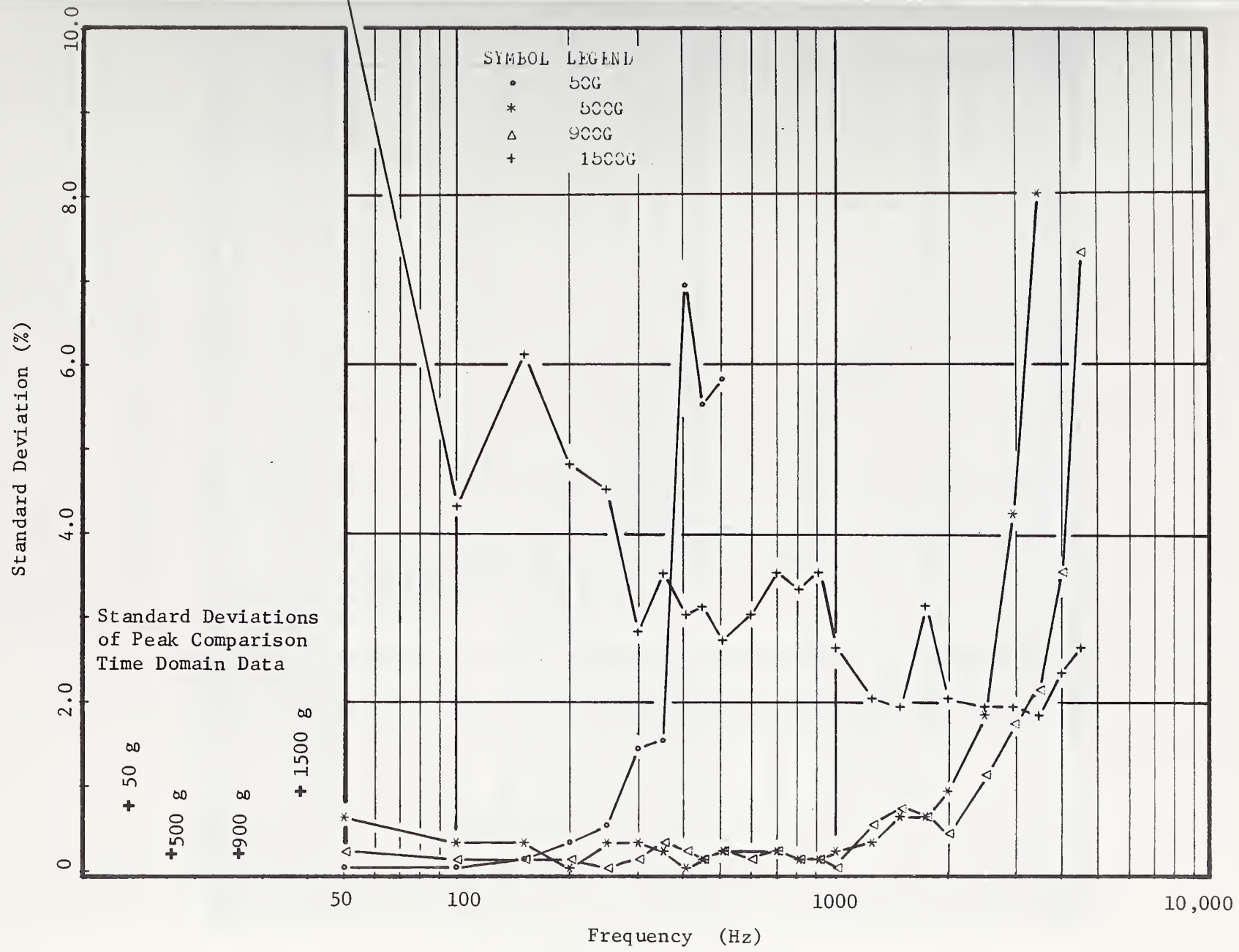

FIGURE 9d. Standard Deviations of Pickup B Sensitivities.

FIGURE 9e. Phase of Pickup A

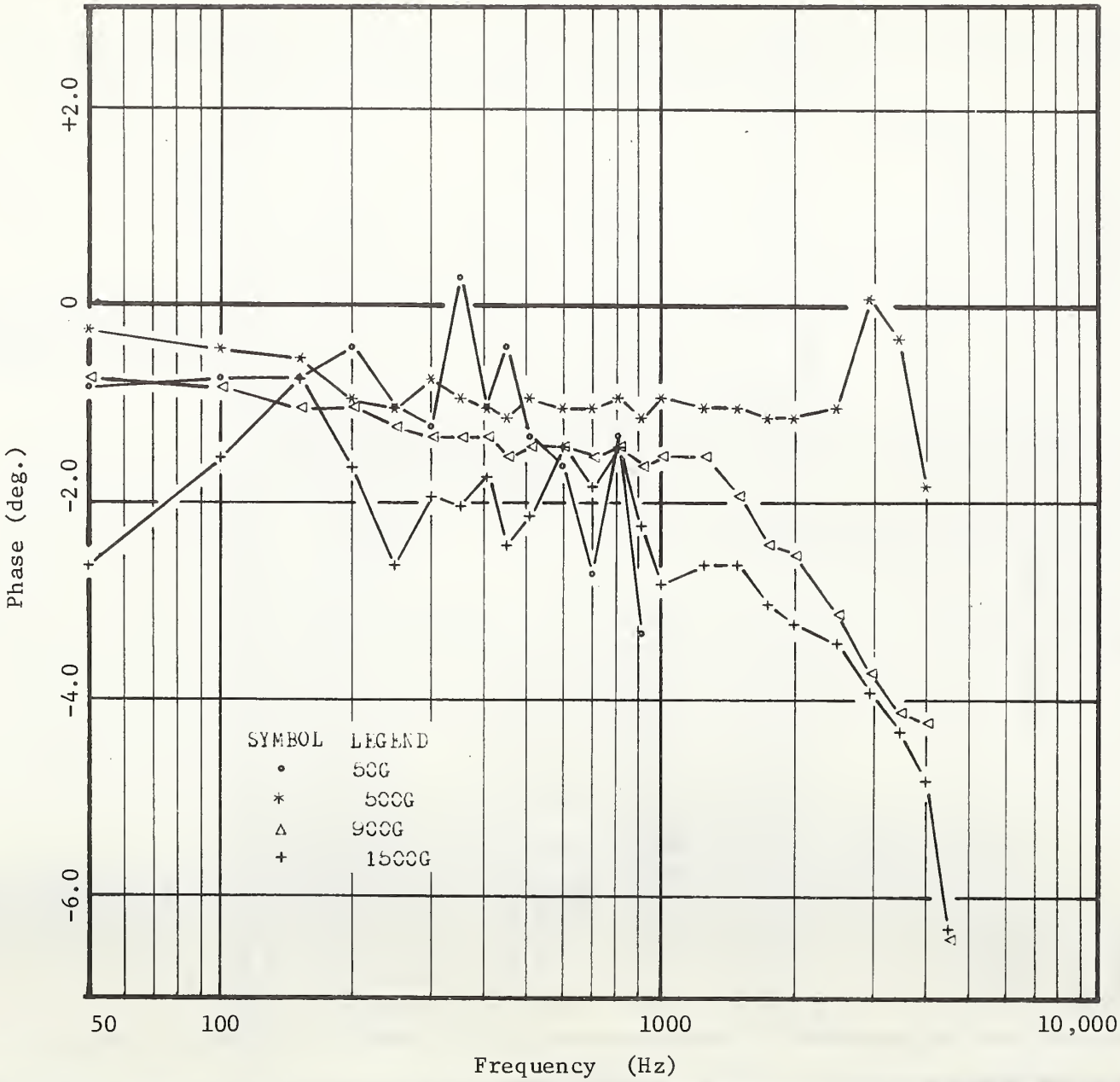

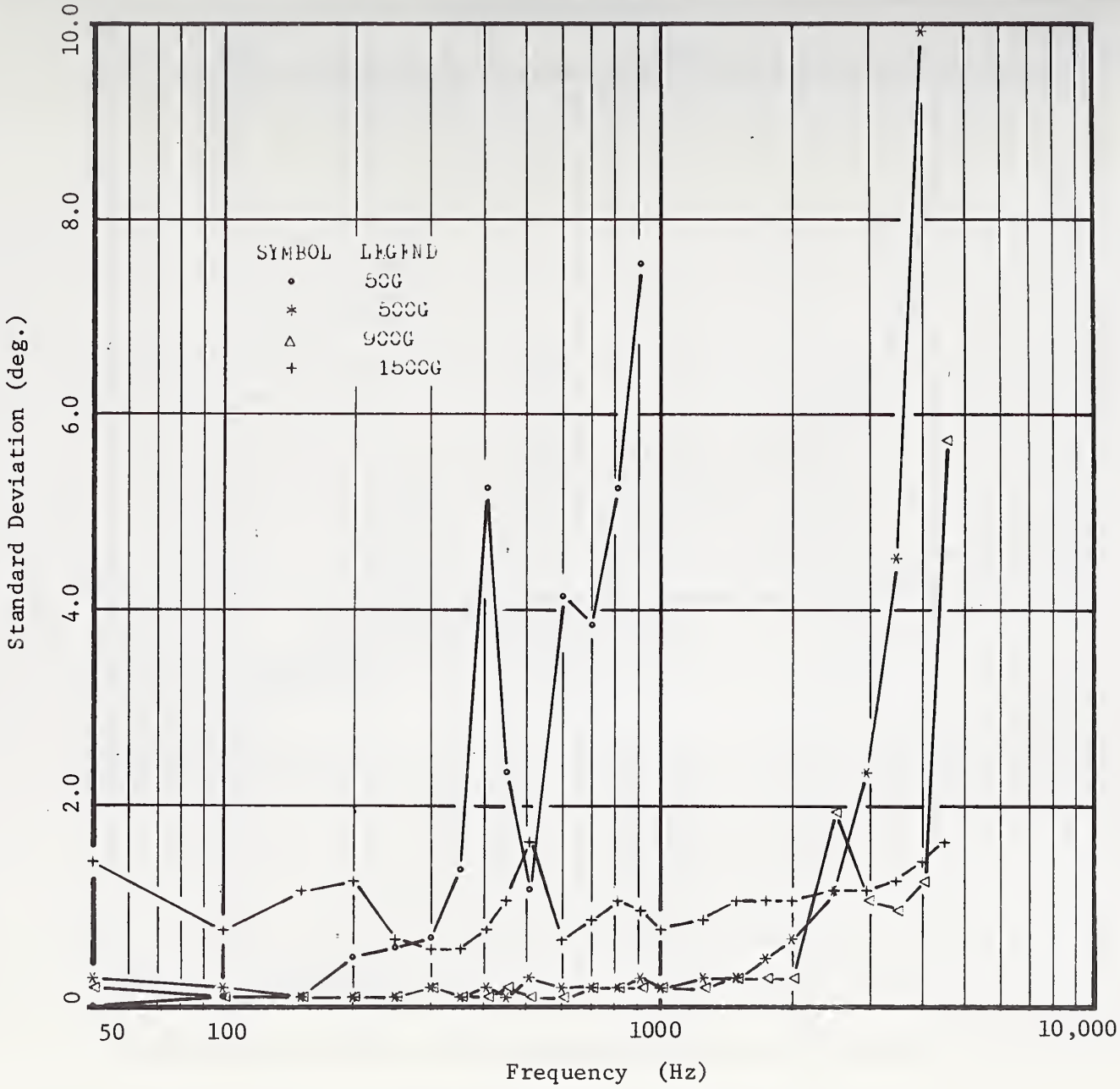

FIGURE 9f. Standard Deviation of Pickup A Phase Data.

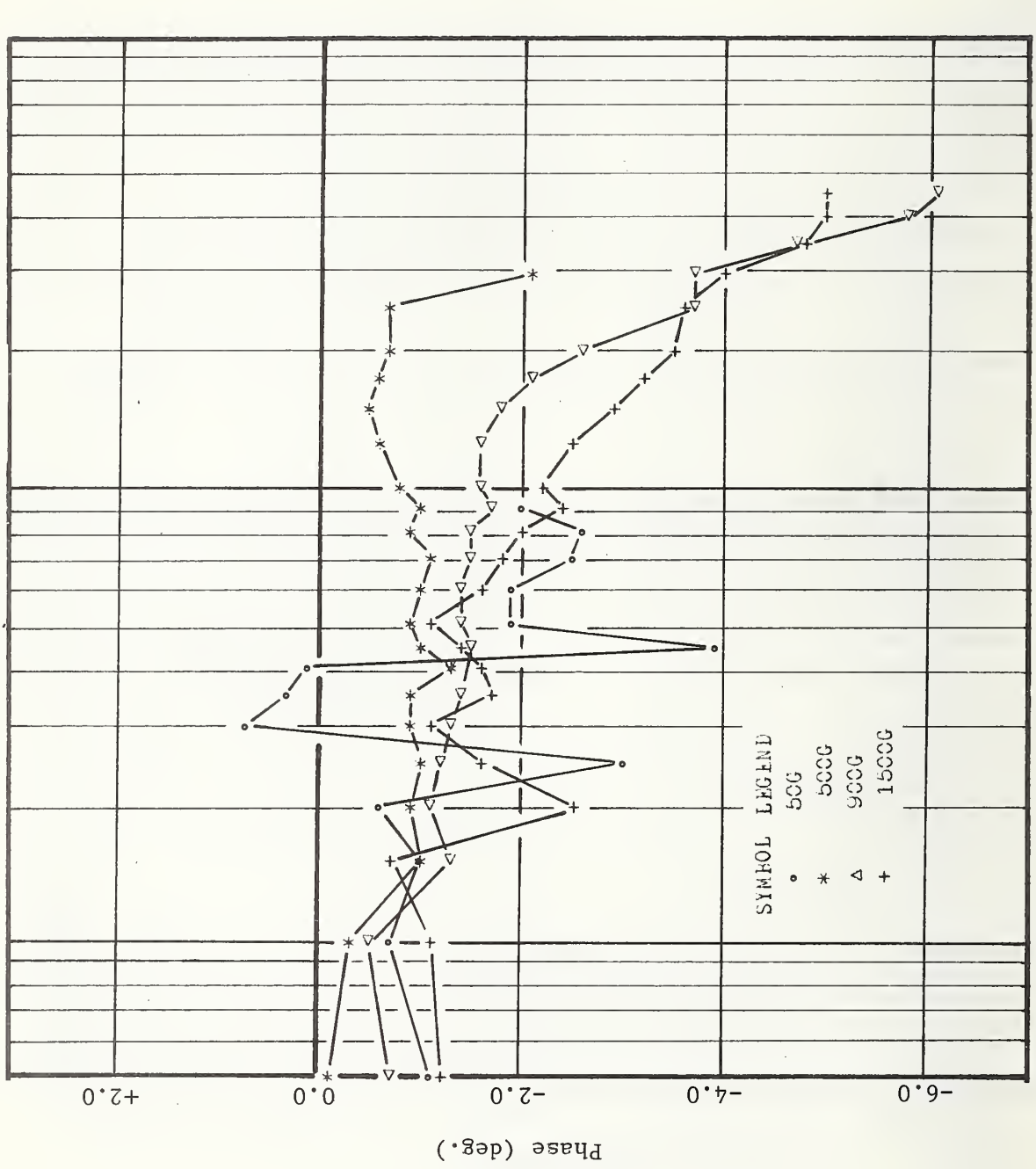

FIGURE 9g. Phase of Pickup B.

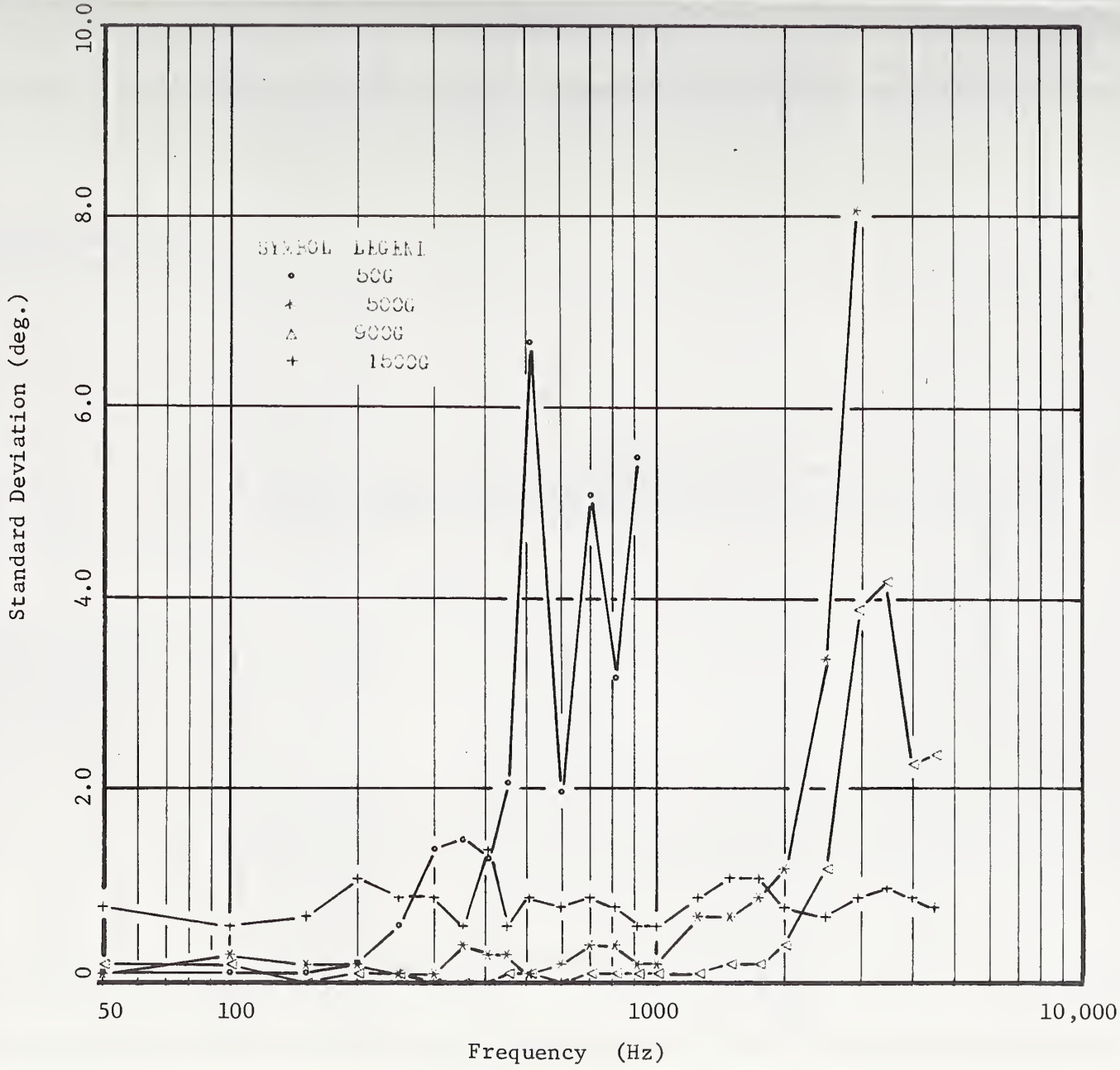

FIGURE 9h. Standard Deviation of Pickup B Phase Data.

FIGURE 10a. Calculated Ratio A/B.

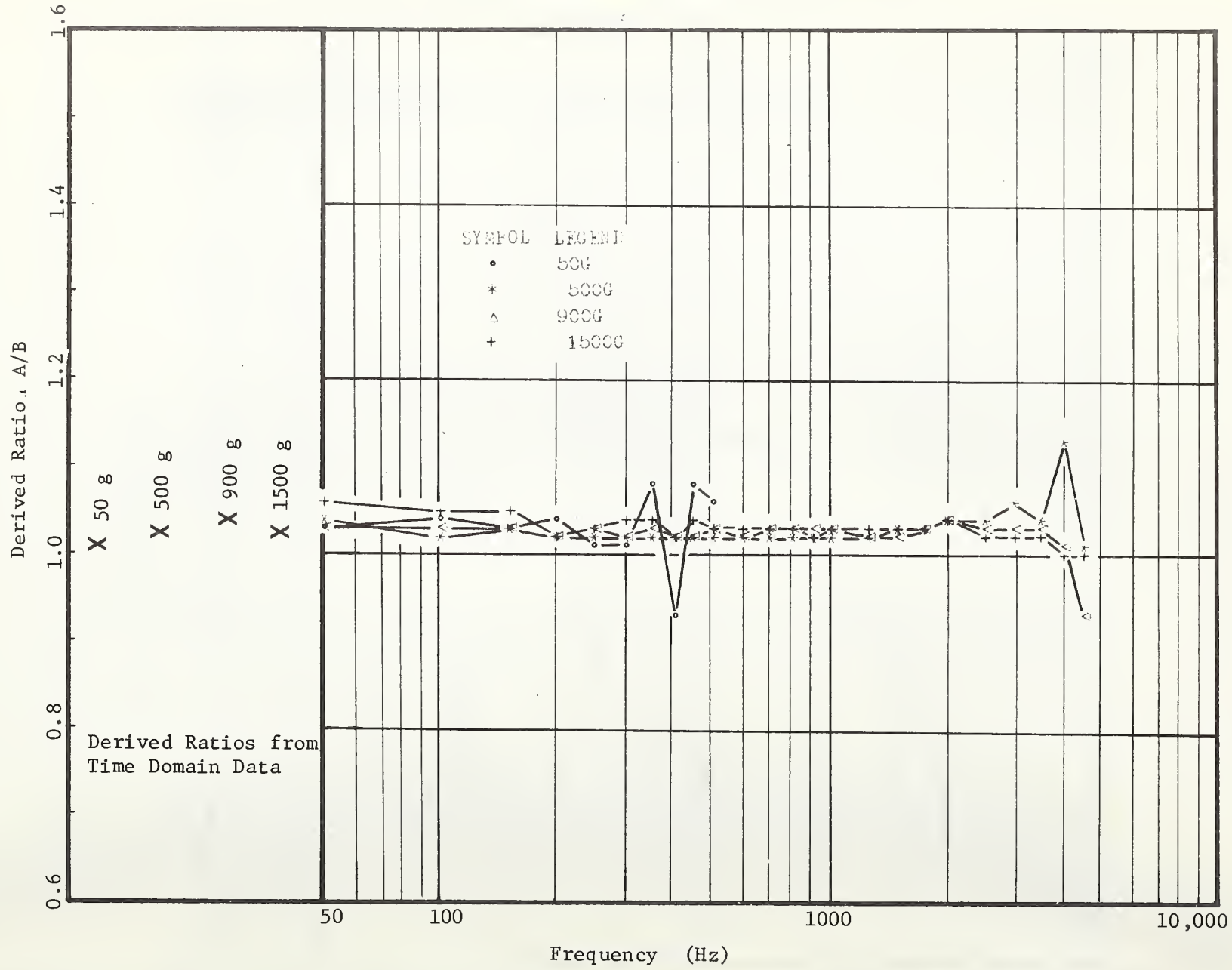

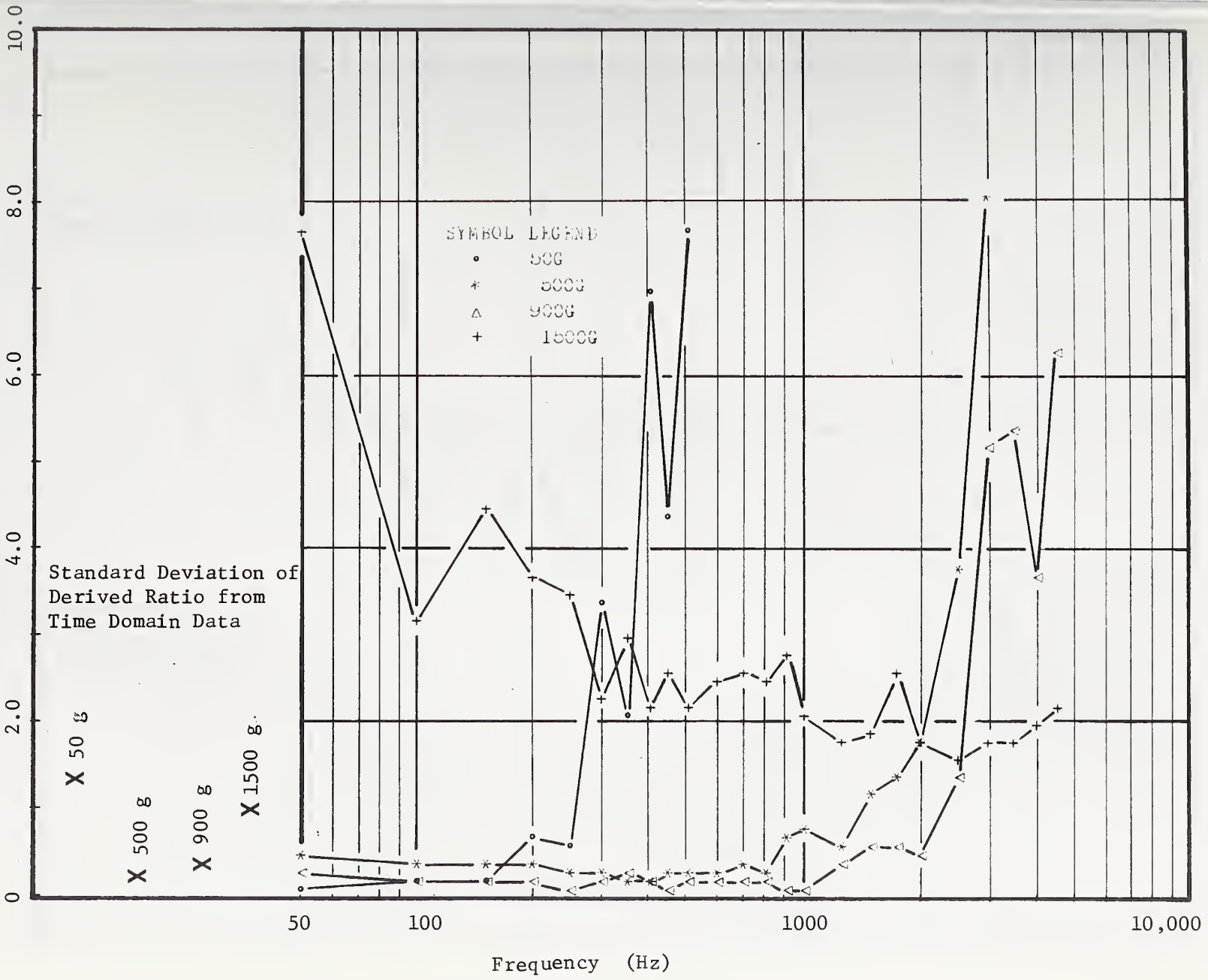

FIGURE 10b. Standard Deviation of Calculated Ratio A/B.

FIGURE 10c. Measured Ratio A/B.

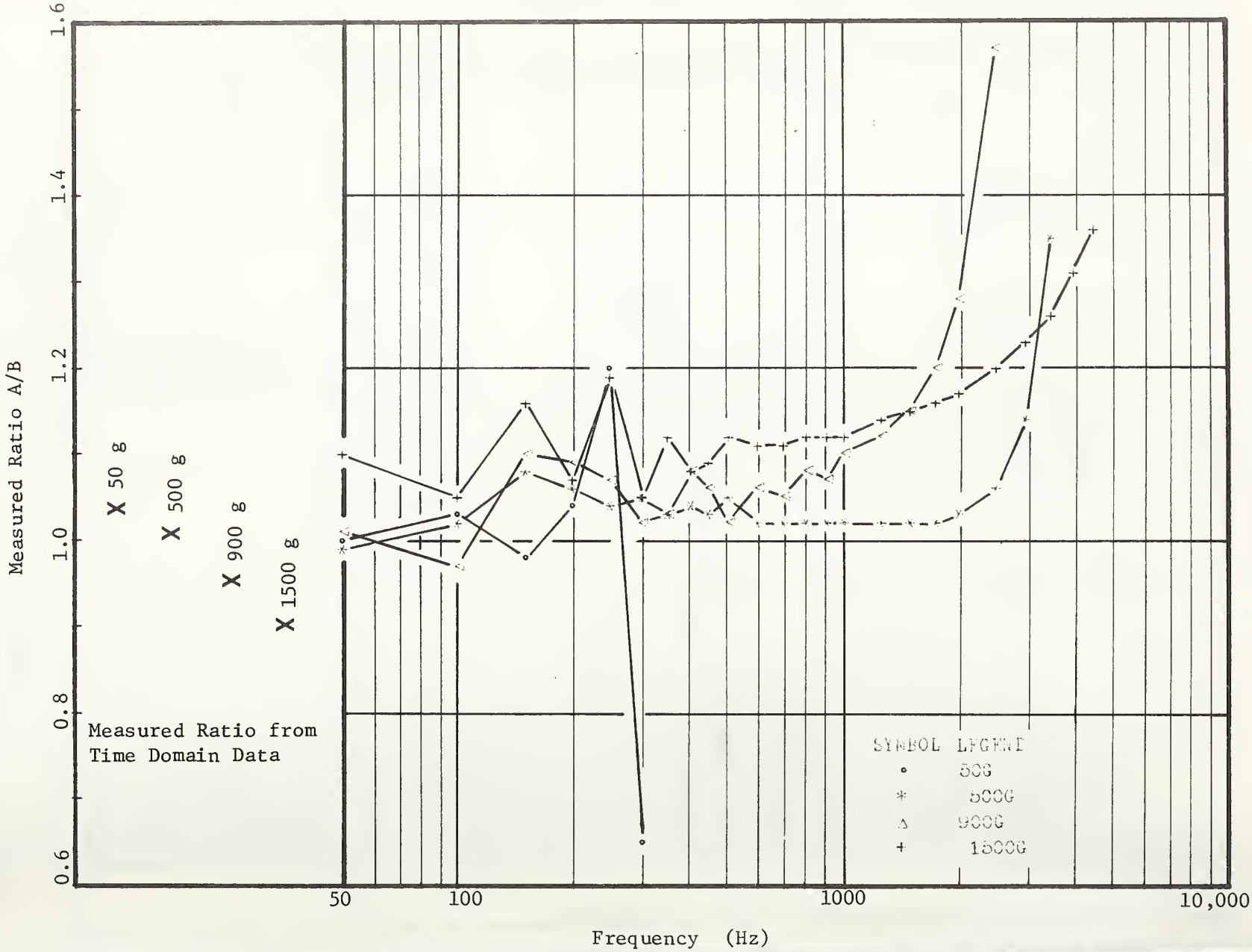

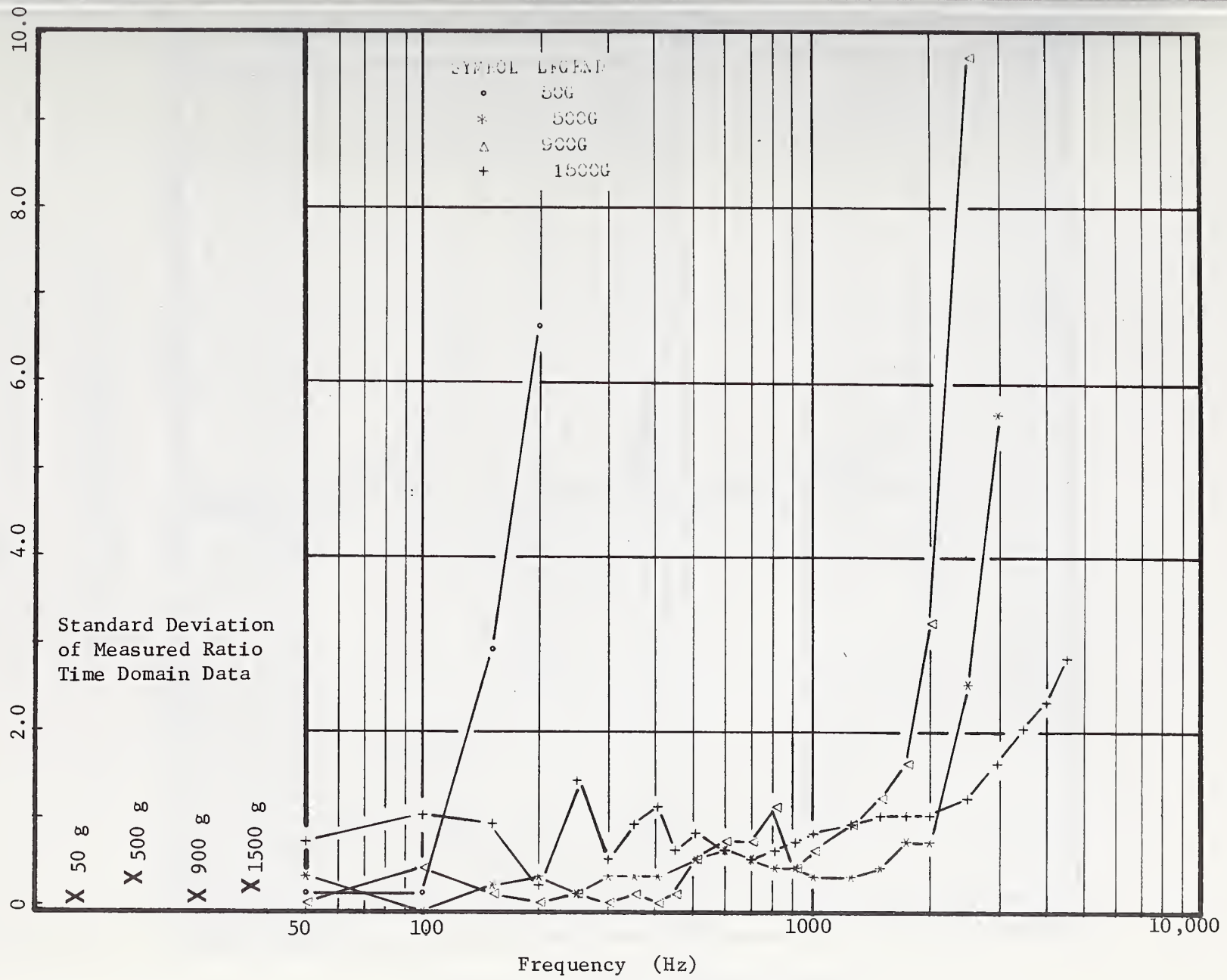

FIGURE 10d. Standard Deviation of Measured Ratio A/B.

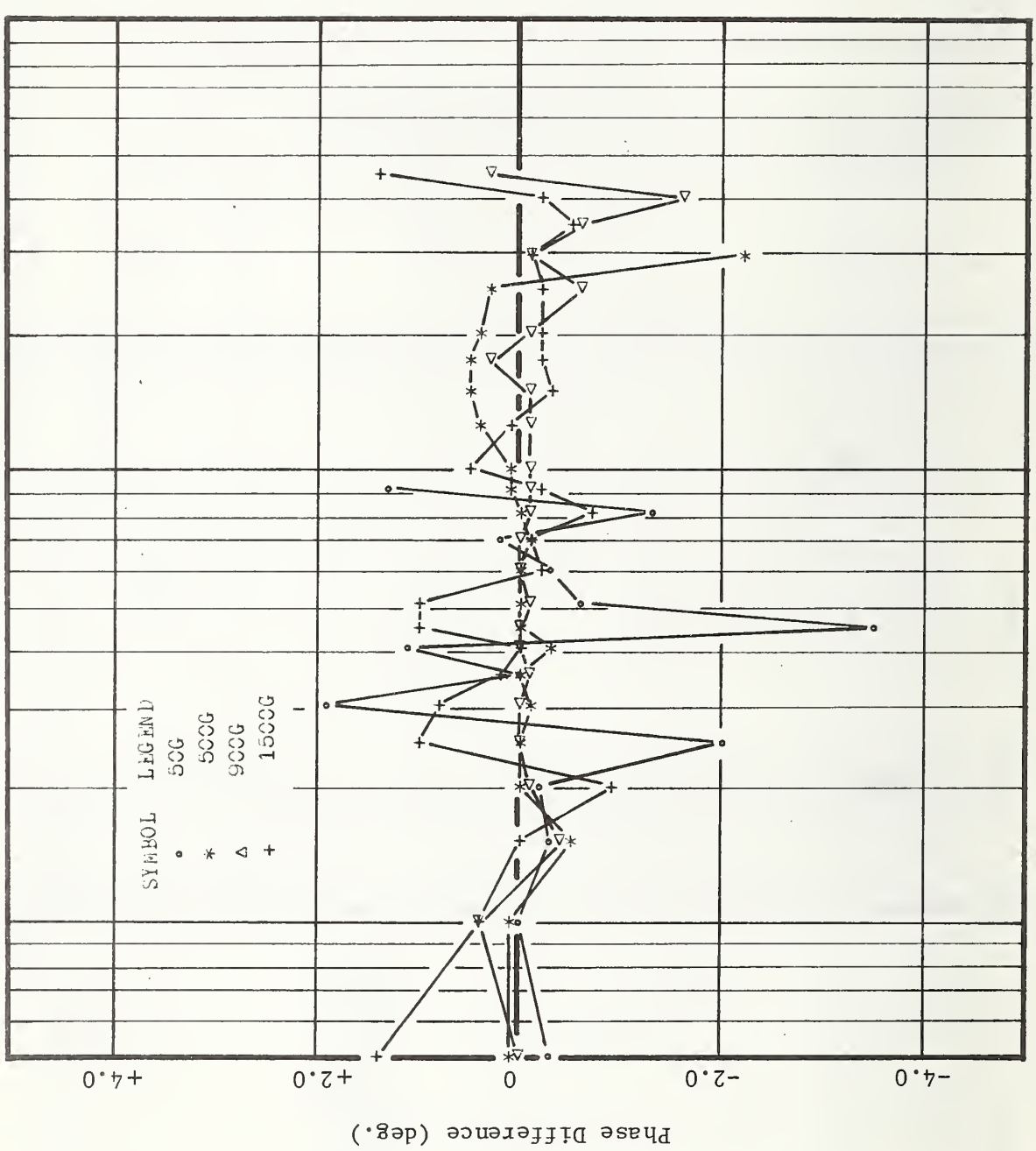

FIGURE 10e. Computed Phase Difference

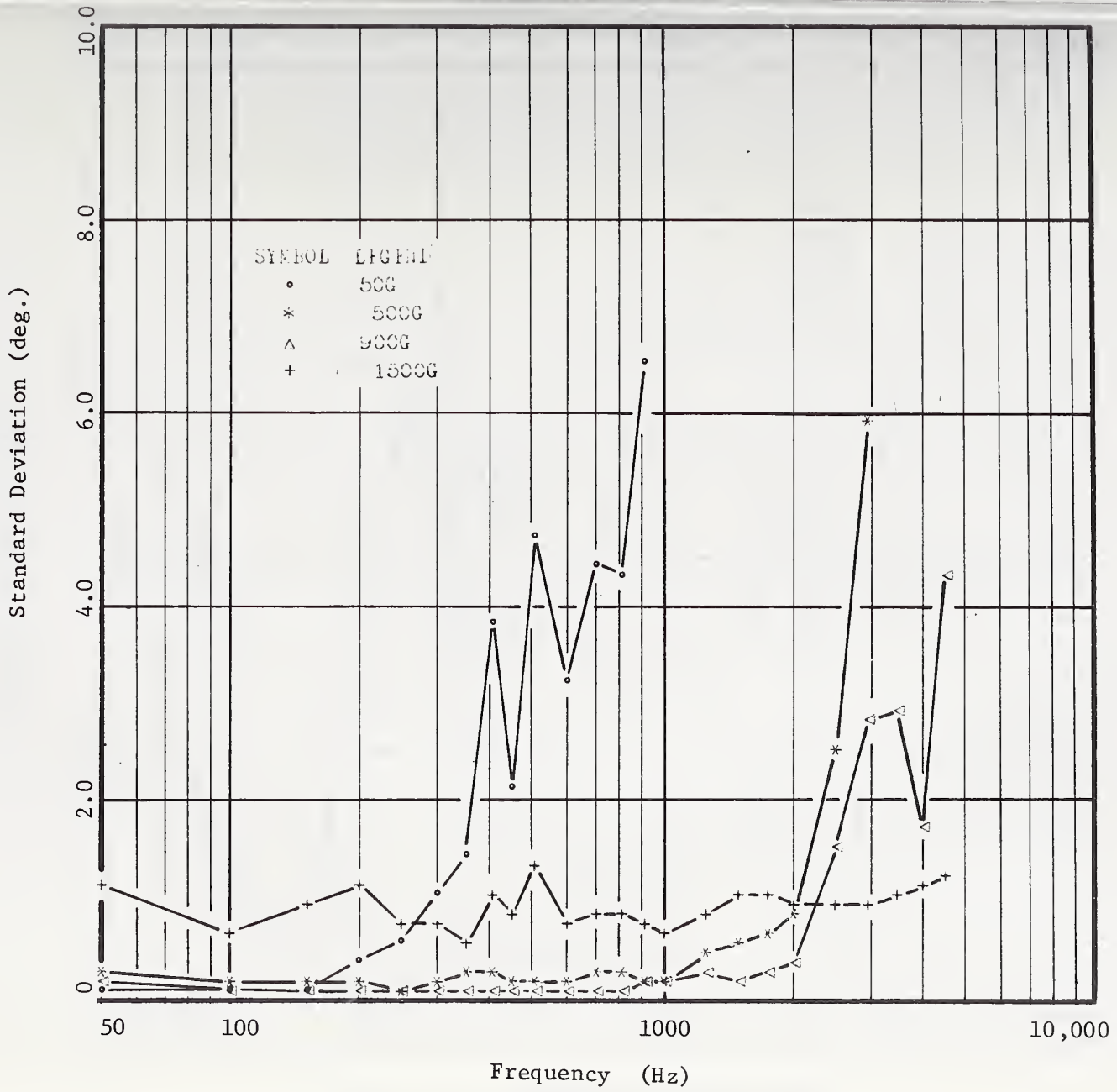

FIGURE 10f. Standard Deviation of Computed Phase Difference.

FIGURE 10g. Measured Phase Difference.

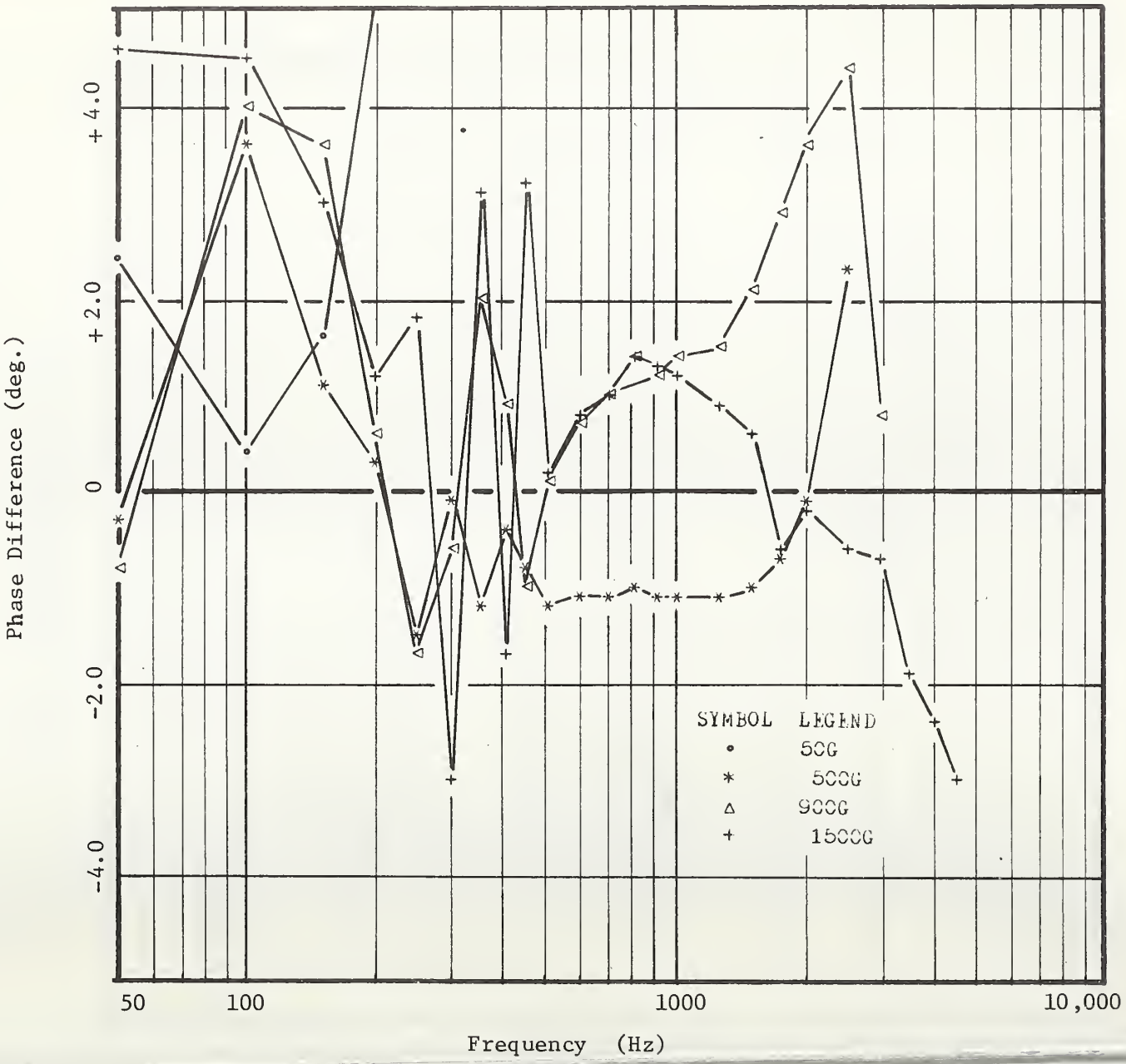

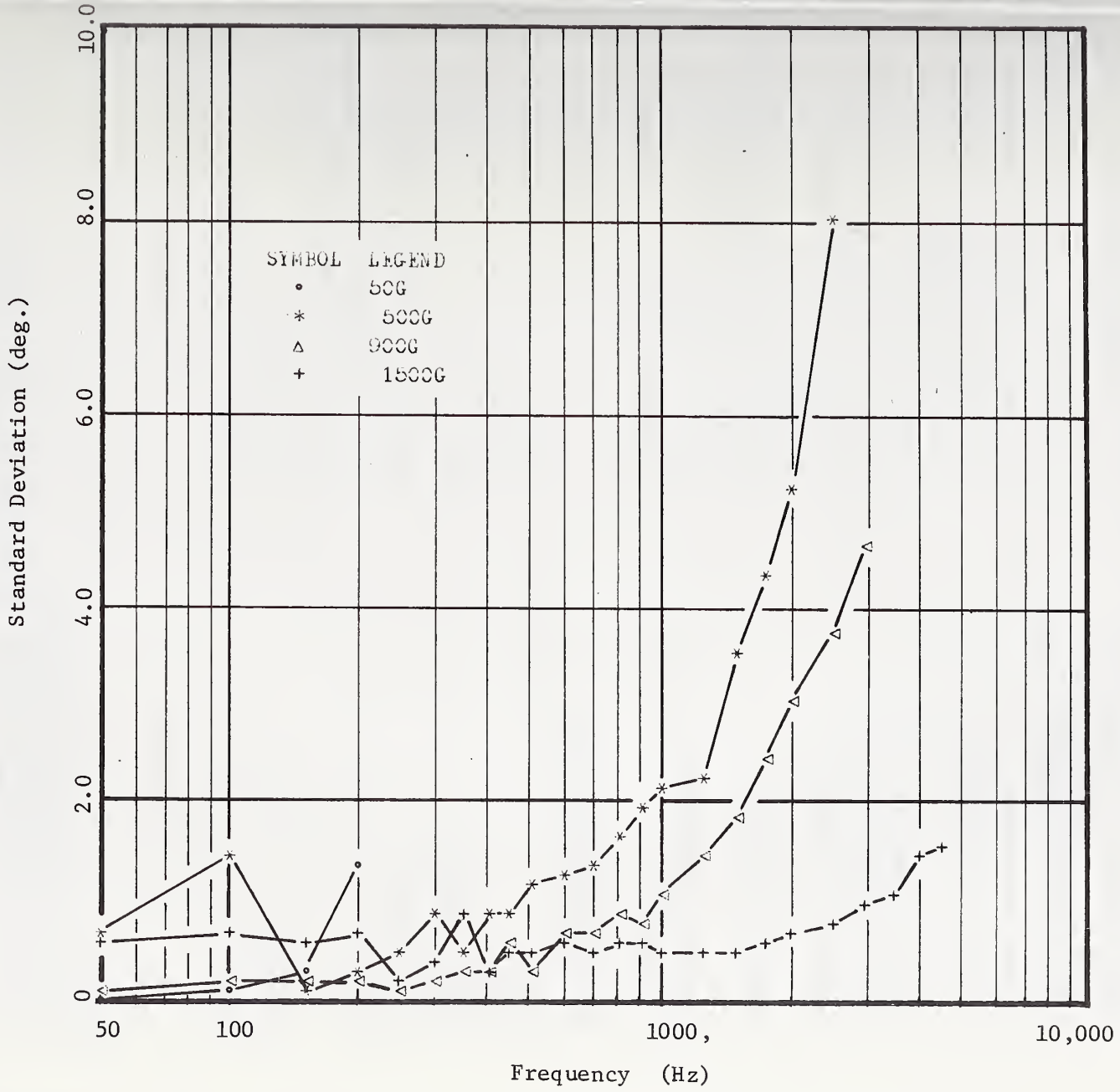

FIGURE 10h. Standard Deviation of Measured Phase Difference.

APPENDIX A

TEST ACCELEROMETER A AND B SPECIFICATIONS

The following specifications were excerpted from the manufacturer's description data sheets. Units of measure are given as stated by the manufacturer.

Dynamic Characteristics

Charge Sensitivity	0.7 pC/g, nominal
Voltage Sensitivity[1]	0.65 mV/g, nominal 0.55 mV/g, minimum
Frequency Response (+10%)[2]	2 to 15,000 Hz
Mounted Resonant Frequency	80,000 Hz, nominal
Transverse Sensitivity	5% maximum, 3% on special selection
Amplitude Linearity	Sensitivity increases approximately 1% per 2000 g, 0 to 20,000 g.
Transducer Capacitance	800 pF, nominal
Resistance	20,000 MΩ minimum, at +25°C

Physical Characteristics

Design	Shear
Weight	13 grams
Crystal Material	PZT
Case Material	300 Series Stainless Steel
Mounting	Hole for 10-32 x 1/8 in., mounting stud. Recommended mounting torque: 18 in-lb.
Grounding	Case grounded
Connector	Coaxial, 10-32 thread

Notes:

[1]With 300 pF external capacitance.
[2]In shock measurements minimum pulse duration for half-sine or triangular pulses should exceed 75 μs to avoid high frequency ringing.

Environmental Characteristics

Acceleration Limit	Shock: ±20,000 g, any direction
Zero Shift	±750 pC, maximum, for 16,000 pk pC output
Base Strain Sensitivity	0.02 equivalent g per microinch per inch, nominal
Temperature	-54°C to +177°C
Altitude	Not affected
Humidity	Epoxy sealed

APPENDIX B

FORTRAN FAST FOURIER TRANSFORM SUBROUTINE

```
C   COMPUTATION OF TRANSFORM
C
C   ARRAY 'DATA' MUST BE IN COMPLEX FORM FOR USE IN SUBROUTINE FFT
C
C   TRANSFORM VALUES ARE RETURNED IN ARRAY 'DATA', REPLACING THE INPUT
C
C   IF AN ISIGN=-1 TRANSFORM IS FOLLOWED BY AN ISIGN=+1 TRANSFORM (OR A
C   ISIGN=+1 BY AN ISIGN=-1),THE ORIGINAL DATA REAPPEAR, MULTIPLIED BY NN
C
C   SUBROUTINE FFT IS A FAST FOURIER TRANSFORM ALGORITHM WHICH IS
C   UTILIZED IN THE CALCULATION OF THE FOURIER TRANSFORM OF A TIME SIGNAL
C
C   THE FOURIER INTEGRAL TRANSFORM IS A MATHEMATICAL OPERATION WHICH
C   DECOMPOSES A TIME SIGNAL, IN THE FORM OF A DATA ARRAY, INTO ITS
C   COMPLEX FREQUENCY COMPONENTS (AMPLITUDE AND PHASE)
C
C
      SUBROUTINE FFT(DATA,NN,ISIGN)
      DIMENSION DATA(1)
      PI2=1.5707963
      N=NN*2
      J=1
      DO 56 I=1,N,2
      IF (I-J) 10,20,20
   10 TEMP=DATA(J)
      TEMI=DATA(J+1)
      DATA(J)=DATA(I)
      DATA(J+1)=DATA(I+1)
      DATA(I)=TEMP
      DATA(I+1)=TEMI
   20 M=N/2
   30 IF(J-M) 50,50,40
```

```
40 J=J-M
   M=M/2
   IF (M-2) 50,30,30
50 J=J+M
55 CONTINUE
   MMAX=2
60 IF (MMAX-N) 70,90,90
70 ISTP=2*MMAX
   DO 80 M=1,MMAX,2
   THET=ISIGN*(M-1)*3.1415927/MMAX
   WR=SIN(THET+PI2)
   WI=SIN(THET)
   DO 80 I=M,N,ISTP
   J=I+MMAX
   TEMR=WR*DATA(J)-WI*DATA(J+1)
   TEMI=WR*DATA(J+1)+WI*DATA(J)
   DATA(J)=DATA(I)-TEMR
   DATA(J+1)=DATA(I+1)-TEMI
   DATA(I)=DATA(I)+TEMR
   DATA(I+1)=DATA(I+1)+TEMI
80 CONTINUE
   MMAX=ISTP
   GO TO 60
90 MMAX=N/2
   RETURN
   END
```

NBS-114A (REV. 7-73)

U.S. DEPT. OF COMM. BIBLIOGRAPHIC DATA SHEET	1. PUBLICATION OR REPORT NO. NBS IR 74-480	2. Gov't Accession No.	3. Recipient's Accession No.

4. TITLE AND SUBTITLE

EVALUATION AND CALIBRATION OF MECHANICAL SHOCK ACCELEROMETERS BY COMPARISON METHODS

5. Publication Date: March 1974

6. Performing Organization Code

7. AUTHOR(S)

John D. Ramboz, Charles Federman

8. Performing Organ. Report No. NBSIR 74-480

9. PERFORMING ORGANIZATION NAME AND ADDRESS

NATIONAL BUREAU OF STANDARDS
DEPARTMENT OF COMMERCE
WASHINGTON, D.C. 20234

10. Project/Task/Work Unit No.

11. Contract/Grant No.

12. Sponsoring Organization Name and Complete Address *(Street, City, State, ZIP)*

Metrology Engineering Center, Bureau of Naval Weapons Representative, Pomona, California 91766; the Aerospace Guidance and Metrology Center, Newark Air Force Station, Newark, Ohio 43055; and the Metrology and Calibration Center, Redstone Arsenal, Alabama 35809

13. Type of Report & Period Covered: Final

14. Sponsoring Agency Code: CCG 72-64

15. SUPPLEMENTARY NOTES

16. ABSTRACT *(A 200-word or less factual summary of most significant information. If document includes a significant bibliography or literature survey, mention it here.)*

A means to calibrate mechanical shock accelerometers by a comparison method has been developed. Detailed procedures and equipment used to generate mechanical shock pulses, collect data, and analyze the results are discussed. Three accelerometers were subjected to haversine acceleration-time pulses of 50, 500, 900 and 1500 g peak amplitudes and time durations of 8.5, 1.2, 1.2, and 0.7 ms, respectively. Both time- and frequency-domain calibrations were performed. The shock calibrations agreed with sinusoidal values to within a few percent. Problems encountered and future developments are discussed.

17. KEY WORDS *(six to twelve entries; alphabetical order; capitalize only the first letter of the first key word unless a proper name; separated by semicolons)*

Accelerometer, calibration, comparison reference, mechanical shock, shock generation, shock pickup, vibration.

18. AVAILABILITY

☐ Unlimited

☒ For Official Distribution. Do Not Release to NTIS

☐ Order From Sup. of Doc., U.S. Government Printing Office Washington, D.C. 20402, SD Cat. No. C13

☐ Order From National Technical Information Service (NTIS) Springfield, Virginia 22151

19. SECURITY CLASS (THIS REPORT)	21. NO. OF PAGES
UNCLASSIFIED	65
20. SECURITY CLASS (THIS PAGE)	22. Price
UNCLASSIFIED	

USCOMM-DC 29042-P